

1 **COVER PAGE**

2

3 **Title:** Cytokinin Signaling is Essential for Organ Formation in *Marchantia polymorpha*

4

5 **Running head (short title):** Cytokinin signaling in *Marchantia*

6

7 **Corresponding author:** M. Umeda; Graduate School of Science and Technology, Nara
8 Institute of Science and Technology, Takayama 8916-5, Ikoma, Nara 630-0192, Japan; Tel.
9 +81-743-72-5592; Fax +81-743-72-5599; E-mail: mumeda@bs.naist.jp

10

11 **Subject areas:** (1) growth and development, (3) regulation of gene expression

12

13 **2 black and white figures, 5 colour figures, 1 table, 1 supplementary material.**

14 **Title:** Cytokinin Signaling is Essential for Organ Formation in *Marchantia polymorpha*

15

16 **Running head (short title):** Cytokinin signaling in *Marchantia*

17

18 Shiori S. Aki¹, Tatsuya Mikami¹, Satoshi Naramoto², Ryuichi Nishihama³, Kimitsune Ishizaki⁴,
19 Mikiko Kojima⁵, Yumiko Takebayashi⁵, Hitoshi Sakakibara^{5,6}, Junko Kyojuka², Takayuki
20 Kohchi³, Masaaki Umeda^{1,*}

21

22 ¹Graduate School of Science and Technology, Nara Institute of Science and Technology,
23 Takayama 8916-5, Ikoma, Nara 630-0192, Japan

24 ²Graduate School of Life Sciences, Tohoku University, Katahira 2-1-1, Aoba-ku, Sendai 980-
25 8577, Japan

26 ³Graduate School of Biostudies, Kyoto University, Kyoto 606-8502, Japan

27 ⁴Graduate School of Science, Kobe University, Kobe 657-8501, Japan

28 ⁵RIKEN Center for Sustainable Resource Science, Suehiro 1-7-22, Tsurumi, Yokohama 230-
29 0045, Japan

30 ⁶Graduate School of Bioagricultural Sciences, Nagoya University, Furo-cho, Chikusa-ku,
31 Nagoya 464-8601, Japan

32

33 ***Corresponding author:** E-mail, mumeda@bs.naist.jp; Fax, +81-743-72-5599

34

35 **Abbreviations:** Aux/IAA, AUXIN/INDOLE-3-ACETIC ACID; ARF, AUXIN RESPONSE
36 FACTOR; BA, 6-benzyladenine; CHK, CASE domain-containing histidine kinase receptor;
37 cZ, cis-zeatin; CKX, cytokinin oxidase; CRF, cytokinin response factor;

38 *EF1 α* , *ELONGATION FACTOR1 α* ; GUS, β -glucuronidase; HPT, histidine-containing;

39 phosphotransfer protein; iP, isopentenyladenine; IPT, isopentenyltransferase; qRT-PCR,

40 quantitative reverse transcription-PCR; RR, response regulator; Tak, Takaragaike; tZ, trans-

41 zeatin.

42 **Abstract**

43 Cytokinins are known to regulate various physiological events in plants. Cytokinin signaling is
44 mediated by the phosphorelay system, one of the most ancient mechanisms controlling
45 hormonal pathways in plants. The liverwort *Marchantia polymorpha* possesses all components
46 necessary for cytokinin signaling; however, whether they respond to cytokinins and how the
47 signaling is fine-tuned remain largely unknown. Here we report cytokinin function in
48 *Marchantia* development and organ formation. Our measurement of cytokinin species revealed
49 that cis-zeatin is the most abundant cytokinin in *Marchantia*. We reduced the endogenous
50 cytokinin level by overexpressing the gene for cytokinin oxidase, MpCKX, which inactivates
51 cytokinins, and generated overexpression and knockout lines for type-A (MpRRA) and type-B
52 (MpRRB) response regulators to manipulate the signaling. The overexpression lines of MpCKX
53 and MpRRA, and the knockout lines of MpRRB, shared phenotypes such as inhibition of gemma
54 cup formation, enhanced rhizoid formation and hyponastic thallus growth. Conversely, the
55 knockout lines of MpRRA produced more gemma cups and exhibited epinastic thallus growth.
56 MpRRA expression was elevated by cytokinin treatment and reduced by knocking out MpRRB,
57 suggesting that MpRRA is upregulated by the MpRRB-mediated cytokinin signaling, which is
58 antagonized by MpRRA. Our findings indicate that when plants moved onto land they already
59 deployed the negative feedback loop of cytokinin signaling, which has an indispensable role in
60 organogenesis.

61

62 **Keywords**

63 Cytokinin, *Marchantia polymorpha*, organogenesis, plant evolution, response regulator

64

65 **Introduction**

66 Cytokinin phytohormones are involved in a broad range of physiological events, such as cell
67 proliferation and differentiation, organ growth, shoot initiation and leaf senescence (Brenner et
68 al. 2005, Kim et al. 2006, Dello Ioio et al. 2008, Kieber and Schaller 2014). Cytokinin signaling
69 is mediated by a phosphorelay system (Kieber and Schaller 2014), which, in *Arabidopsis*
70 *thaliana*, consists of CHASE domain-containing histidine kinase receptors (CHKs), histidine-
71 containing phosphotransfer proteins (HPTs) and response regulators (RRs). Cytokinin
72 perception by CHKs at the plasma and endoplasmic reticulum membrane induces
73 autophosphorylation of CHKs, followed by phosphate transfer to cytosolic HPTs. After moving
74 into the nucleus, HPTs transfer the phosphate to type-B RR, which are then activated and
75 function as transcription factors to regulate the expression of target genes (Hwang and Sheen
76 2001, Sakai et al. 2001, Taniguchi et al. 2007). Among these target genes are type-A RRs,
77 which negatively control cytokinin signaling by competing with type-B RRs for phosphate
78 transfer (To et al. 2004, 2007). *Arabidopsis* RRs (ARRs) include 11 type-B members, among
79 which ARR1, ARR10 and ARR12 play a predominant role in cytokinin signaling. The triple
80 mutant largely lacks cytokinin-dependent gene expression, and exhibits retarded shoot growth,
81 aborted primary root growth and seed enlargement (Argyros et al. 2008, Ishida et al. 2008,
82 Mason et al. 2005). Although functional redundancy of RRs gives robustness in cytokinin
83 signaling against various perturbations during plant development (Choi et al. 2014), it also
84 complicates the unraveling of downstream events. For instance, how cytokinins control cell
85 proliferation remains largely unknown. Previous studies demonstrated that *Arabidopsis cyclin*
86 *D3* (*CYCD3*) is upregulated by cytokinins, and that its overexpression enables callus formation
87 on auxin-treated leaf explants in the absence of exogenous cytokinins (Soni et al. 1995, Riou-

88 Khamlichi et al. 1999). Therefore, it was hypothesized that *CYCD3* plays a major role in
89 cytokinin-triggered cell proliferation; however, which and how ARRs control *CYCD3*
90 expression and to what extent *CYCD3* contributes to cytokinin action on the cell cycle are still
91 elusive.

92 The liverwort *Marchantia polymorpha* is a model basal land plant (Ishizaki et al.
93 2016, Shimamura 2016). The organization of the thalloid body originates from highly regulated
94 division of the apical cell and its descendants at the notch, which is located at the tip of the
95 thallus. Gemma cups accommodating numerous multicellular clones, gemmae, are produced
96 on the dorsal side of the thallus along the midrib. On the ventral side are many tubular cells
97 called rhizoids, which absorb water and nutrients from the soil. A recent genome and
98 transcriptome project revealed a low redundancy of regulatory genes in *Marchantia* (Bowman
99 et al. 2017); for instance, those related to auxin signaling are one gene for TRANSPORT
100 INHIBITOR RESPONSE 1 (TIR1) receptor, one for AUXIN/INDOLE-3-ACETIC
101 ACID (Aux/IAA) protein, and three for AUXIN RESPONSE FACTOR (ARF) (Flores-
102 Sandoval et al. 2015, Kato et al. 2015). Previous studies demonstrated that an F-box-mediated
103 pathway controls the signaling of auxin, gibberellin, jasmonic acid and strigolactone, and that
104 the phosphorelay system governs cytokinin and ethylene signaling (Wang and Irving 2011).
105 Phylogenetic analyses revealed that the components of the F-box-mediated pathway mostly
106 exist in *Marchantia*, but not in charophyte green algae, suggesting that F-box-mediated
107 hormonal signaling was born when plants moved onto land (Bowman et al. 2017). On the other
108 hand, the phosphorelay system exists in charophytes as well as in *Marchantia*, implying that it
109 is more ancient than the F-box-mediated system (Bowman et al. 2017). *Marchantia* is thus a

110 good model organism to understand basic functions of the major hormonal signaling systems
111 in the earliest divergent lineages of extant land plants.

112 The *Marchantia* genome encodes all essential components of cytokinin signaling,
113 namely two CHKs (MpCHKs), one HPT (MpHPT), and one for each type-A RR (MpRRA) and
114 type-B RR (MpRRB) (Bowman et al. 2017). One of the two MpCHKs was shown to bind to
115 cytokinins *in vitro*, although its binding activity to all tested cytokinins was lower than those of
116 *Arabidopsis* and *Physcomitrella patens* (Gruhn et al. 2014). Flores-Sandoval et al. (2016)
117 reported that microRNA-mediated knockdown of MpRRB and overexpression of MpRRA
118 caused defects in thallus development, generating smaller thalli with ectopic serration on
119 margins and fewer gemma cups. However, a low level of MpRRB transcripts remained in the
120 knockdown lines, and no statistical analysis was performed for the MpRRA-overexpressing
121 lines. Moreover, cytokinin dependency of the observed phenotype was assessed by treatment
122 of the Mprrb knockdown lines with a high dose (40 μ M) of 6-benzyladenine (BA); therefore,
123 the involvement of response regulators in cytokinin signaling and their role in *Marchantia*
124 development still remain elusive. Here we investigate biological functions of cytokinins in
125 *Marchantia* by distorting hormone levels and signaling. Our results indicate that cytokinins
126 control gemma cup and rhizoid formation, and thallus growth, through the MpRRB-mediated
127 pathway, which is antagonized by MpRRA, suggesting that cytokinin signaling mediated by
128 the phosphorelay system already participated in crucial developmental processes when plants
129 moved onto land.

130

131 **Results**

132 **cZ-type cytokinins are abundant in *Marchantia***

133 We first examined the response of *Marchantia* to exogenously applied cytokinins. Since
134 gemmae formed in gemma cups are not equal in developmental stages, we grew wild-type (Tak-
135 1) gemmae on cytokinin-free agar medium for 6 days, then individuals were transferred to agar
136 medium containing isopentenyladenine (iP), trans-zeatin (tZ), cis-zeatin (cZ) or BA and grown
137 for 21 days. At a concentration of 10 μ M, none of the tested cytokinins affected thallus size,
138 gemma cup number or lobe number, and cZ and BA reduced the number of gemmae produced
139 in gemma cups (Supplementary Fig. S1). At 50 μ M, iP severely inhibited thallus growth,
140 thereby making it difficult to count the lobe number (Supplementary Fig. S2B, D); BA also
141 impaired thallus growth, and BA and cZ inhibited gemma cup formation and gemma production,
142 while tZ did not exert any significant effect (Supplementary Fig. S2). Considering that 1 μ M
143 cytokinins are sufficient to retard shoot and root growth in *Arabidopsis* (To et al. 2004), the
144 observed phenotypes are likely defects caused by excessive amounts of cytokinins in the culture
145 medium.

146 Cytokinin measurements using one-week-old wild-type (Tak-1) thallus revealed that
147 the total amount of tZ, cZ and iP, including riboside and phosphoriboside precursors and
148 glucosides, was 115 pmol/g fresh weight, which is higher than that in *Arabidopsis* shoots and
149 roots (approximately 50 pmol/g fresh weight) (Ko et al. 2014). Interestingly, cZ-type cytokinins
150 were more abundant than tZ- and iP-types, which are major cytokinin species in *Arabidopsis*
151 (Table 1). Three-week-old thalli contained higher amounts of cZ- and iP-type cytokinins in the
152 apical part than in the basal part (Table 1).

153

154 **Cytokinins are required for thallus growth and gemma cup formation**

155 Since the cytokinin level is relatively high in *Marchantia*, as described above, we examined the
156 phenotype when endogenous cytokinins were decreased by overexpressing cytokinin oxidase
157 (CKX), which inactivates cytokinins (Schmülling et al. 2003). One of the two *Marchantia*
158 CKXs, MpCKX2 (Mapoly0093s0012), which shows 61% identity to *Arabidopsis* CKX1, was
159 overexpressed under the constitutive promoter of *ELONGATION FACTOR1 α* (MpEF1 α)
160 (Althoff et al. 2014). We isolated twelve independent lines that showed the same phenotype;
161 therefore, the representative lines #7 and #9 with different MpCKX2 expression levels were
162 used for further analyses (Fig. 1A). The endogenous cytokinin level was reduced in both lines,
163 although more significantly in #7; in one-week-old thalli, tZ was below the quantification limit
164 in both lines, and cZ was 2.6% and 5.2% in #7 and #9, respectively, of that in wild-type (Table
165 1). Both lines formed smaller thalli that bent upward and excessive rhizoids (Fig. 1B, C). The
166 number of gemma cups per unit thallus area was reduced to less than half in #7, and almost no
167 gemma cups were formed in #9 (Fig. 1D; Supplementary Fig. S3). These results indicate that
168 in *Marchantia*, cytokinins are required for thallus growth and gemma cup formation, and inhibit
169 rhizoid formation.

170 In *Marchantia*, all tissues in the thallus body are derived from four merophytes
171 (dorsal, ventral and two lateral merophytes) that surround the single apical cell at the apical
172 notch (Shimamura 2016). Gemma cups are produced very close to the apical cell; cells that are
173 destined to form the gemma cup do not undergo periclinal divisions, and can thus be identified
174 as a set of cylindrical cells that constitute the gemmiparous area just a few cells above the apical
175 cell (Fig. 1E) (Barnes and Land 1908). When 3D images of the apical notch in 10-day-old thalli
176 were reconstructed, we identified the gemmiparous area in 45% of wild-type notches (n = 22),
177 but only in 10% of the MpCKX2-overexpressing line #7 (n = 10); in line #9, no gemmiparous

178 cells were observed (n = 12) (Fig. 1E). These results suggest that cytokinins are required for
179 the initial process of gemma cup formation at the apical notch.

180

181 **Cytokinin signaling components in *Marchantia***

182 In the previous study, Mapoly0022s0150 (CUFF.5443) and Mapoly0101s0006 (CUFF.16381)
183 were identified as MpRRA and MpRRB, respectively (Bowman et al. 2017). However, we
184 noticed that the nucleotide sequences with Mapoly and CUFF numbers, which correspond to
185 the genomic and cDNA sequences, respectively, were not identical for either type-A or -B RRs,
186 probably due to sequencing errors in Mapoly that arose during the genome project. Since the
187 cDNAs that we obtained from wild-type Tak-1 were the same as those predicted from
188 CUFF.5443 and CUFF.16381, we designated CUFF.5443 and CUFF.16381 as MpRRA and
189 MpRRB, respectively. MpRRA encodes a polypeptide of 243 amino acids, and the receiver
190 domain has 64% identity to that of ARR5 (Fig. 2A). MpRRB shows 71% and 84% identity to
191 ARR2 in the receiver domain and the GARP motif, respectively (Fig. 2B). MpRRB possesses
192 a glutamine- and proline-rich C-terminal region, as do type-B RRs, although its length is
193 shorter than that in ARR2 (Fig. 2B).

194 The *Marchantia* genome encodes two cytokinin receptors, MpCHK1
195 (Mapoly0075s0066) and MpCHK2 (Mapoly0104s0036), and one HPT, MpHPT
196 (Mapoly0091s0072) (Bowman et al. 2017). MpCHK1 and MpCHK2 have the conserved
197 cytokinin receiver (CHASE) and histidine kinase domains as well as the receiver and receiver-
198 like domains (Fig. 2C). The amino acid sequences in the histidine kinase domain show a higher
199 similarity between MpCHK1 and MpCHK2 (62%) than between MpCHK1 and the *Arabidopsis*
200 cytokinin receptor AHK4 (44%) (Fig. 2C). MpHPT is closely related to AHP1, with 62%

201 identity in the HPT domain that functions as a phospho-transmitter, and has an N-terminal
202 extension (Fig. 2D) (Suzuki et al. 1998). These results indicate that all components of cytokinin
203 signaling in *Marchantia* are well conserved in essential domains as compared to *Arabidopsis*
204 orthologs.

205

206 **MpRRA and MpRRB are expressed in the notch, the midrib and gemma cups**

207 To further understand the functional role of cytokinin signaling in *Marchantia*, we examined
208 the expression pattern of MpRRA and MpRRB. Quantitative reverse transcription-PCR (qRT-
209 PCR) was conducted using total RNA from young thalli without gemma cups, mature thalli
210 with gemma cups, antheridiophores and archegoniophores. As shown in Fig. 3A and B,
211 transcript levels of MpRRA and MpRRB were higher in mature thalli than in younger plants,
212 and MpRRB was highly expressed at the reproductive stage.

213 We then generated β -glucuronidase (*GUS*) reporter lines: the 5-kb promoter regions
214 of MpRRA and MpRRB were fused to the *GUS* gene, and introduced into wild-type plants. Ten
215 and seven lines of *proMpRRA:GUS* and *proMpRRB:GUS*, respectively, were generated, and
216 both showed the same *GUS* expression patterns among independent lines; therefore, we
217 hereafter show the results of a representative line for each of MpRRA and MpRRB. In
218 *proMpRRA:GUS*, *GUS* signals were not detected in gemmae (Fig. 3C), but appeared in the
219 notch of 5-day-old thalli (Fig. 3D). The signals became stronger in the midrib during thallus
220 growth (Fig. 3E-G), and in 20-day-old plants a high level of *GUS* expression was also observed
221 in gemma cups and developing gemmae (Fig. 3H). *proMpRRB:GUS* showed a similar
222 expression pattern to that of *proMpRRA:GUS*, except that *GUS* signals in the midrib almost
223 disappeared in 20-day-old thalli (Fig. 3M-R). At the reproductive stage, the promoter activities

224 of *MpRRA* and *MpRRB* were detected in whole tissues, but at a reduced level in stalks (Fig. 3I-
225 L, S-V).

226

227 ***MpRRB* is indispensable for gemma cup formation and restricts the number of rhizoids**

228 To elucidate the physiological function of the *MpRRB*-mediated pathway, we knocked out
229 *MpRRB* by inserting the hygromycin phosphotransferase gene using homologous
230 recombination-based gene targeting (Fig. 4A) (Ishizaki et al. 2013), and obtained three
231 independent lines, #194, #307 and #342. Semi-quantitative RT-PCR analysis showed that all
232 three lines lacked the full-length *MpRRB* transcript (Fig. 4B; Supplementary Fig. S4A). Since
233 they exhibited the same phenotype (Fig. 4C; Supplementary Fig. S4B), we used #307 as a
234 representative line for further analysis. Thalli bent diagonally upward and had no gemma cups
235 (Fig. 4C, D). Moreover, numerous rhizoids were formed on the ventral side as observed in
236 *MpCKX2*-overexpressing lines (Figs. 1B, 4C). These phenotypes were suppressed by
237 expressing *MpRRB* under its own promoter (Fig. 4B, C, D). Our results suggest that *MpRRB*
238 is indispensable for proper development of the thallus and gemma cups, and that rhizoid
239 formation is inhibited by the *MpRRB*-mediated pathway.

240 We also generated *MpRRB*-overexpressing lines using the *MpEF1 α* promoter. We
241 transformed 330 pieces of thalli and obtained only one line expressing *MpRRB* at a higher level
242 (3.2-fold) than wild-type (Supplementary Fig. S5A). Thalli of the overexpression line were
243 heavily curled, making it difficult to evaluate the effect of overexpression on gemma cup and
244 rhizoid formation (Supplementary Fig. S5B). This suggests that constitutive overexpression of
245 *MpRRB* causes severe developmental defects in *Marchantia*.

246

247 **MpRRA inhibits MpRRB-mediated cytokinin signaling**

248 We next observed the phenotype of *Mprra* knockout lines. We obtained three independent lines
249 (#288, #289 and #397) by homologous recombination-based gene targeting (Fig. 5A), and
250 found that all expressed no *MpRRA* transcript (Fig. 5B; Supplementary Fig. S6A). Because the
251 three lines exhibited the same phenotype (Fig. 5C; Supplementary Fig. S6B), we present the
252 data for the representative line #289. As shown in Fig. 5C and D, thalli curled downward, and
253 the number of gemma cups per unit thallus area was higher than in wild-type. Such phenotypes
254 were suppressed by expressing *MpRRA* under its own promoter (Fig. 5B, C, D). These data
255 suggest that *MpRRA* plays an inhibitory role in gemma cup formation. We also observed rhizoid
256 formation on the ventral side of thalli, but found no difference between wild-type and *Mprra*
257 knockout lines, suggesting that the sensitivity to cytokinins in rhizoid formation is lower than
258 that in gemma cup formation.

259 To further examine the function of *MpRRA* in *Marchantia* development, we
260 generated twelve independent lines overexpressing *MpRRA* under the *MpEF1 α* promoter.
261 Among them, we analyzed the representative lines #1 and #4, in which the *MpRRA* transcript
262 level increased more than 12- and 44-fold, respectively, compared to wild-type (Fig. 6A). Both
263 lines produced thalli bending upward and numerous rhizoids, while gemma cup formation was
264 severely inhibited (Fig. 6B, C). These phenotypes were similar to those observed in the
265 *MpCKX2*-overexpressing lines and the *Mprrb* knockout lines (Figs. 1, 4), suggesting that
266 *MpRRA* has an antagonistic function to *MpRRB*-mediated cytokinin signaling, which controls
267 proper thallus development, promotes gemma cup formation, and suppresses rhizoid formation.

268 Our qRT-PCR analysis revealed that the *MpRRA* transcript level was lower in the
269 *MpCKX2*-overexpressing lines than in wild-type, and was increased by 50 μ M tZ treatment of

270 wild-type plants for 2 h (Fig. 7A, B). This suggests that *MpRRA* is responsive to cytokinins at
271 the mRNA level, as is the case with *Arabidopsis* type-A RRs (Hwang and Sheen 2001, Sakai
272 et al. 2001, Taniguchi et al. 2007). In the *Mprrb* knockout line, the *MpRRA* mRNA level was
273 lower than that in wild-type (Fig. 7B), while it was 1.7-fold higher in the *MpRRB*-
274 overexpressing line (Fig. 7C). Moreover, tZ-triggered induction of *MpRRA* was completely
275 suppressed in the *Mprrb* knockout line (Fig. 7B). This and results presented above suggest that
276 cytokinins upregulate *MpRRA* through *MpRRB*, whose function is suppressed by *MpRRA*,
277 thereby generating negative feedback.

278

279 **Discussion**

280 In this study, we demonstrated that *Mprrb* knockout lines and overexpression lines of *MpRRA*
281 and *MpCKX2* shared the phenotypes of upward bending of thalli, formation of numerous
282 rhizoids, and defects in gemma cup formation (Figs. 1B, D, 4C, D, 6B, C). In contrast, *Mprra*
283 knockout lines exhibited downward bending of thalli and enhanced gemma cup formation (Fig.
284 5C, D). Moreover, our measurement of *MpRRA* mRNA levels indicated that *MpRRA*
285 expression is upregulated by cytokinins in an *MpRRB*-dependent manner (Fig. 7). These data
286 suggest that *MpRRB*-mediated cytokinin signaling promotes gemma cup formation, inhibits
287 rhizoid formation, controls epinastic thallus growth, and induces *MpRRA* to give negative
288 feedback as is known in *Arabidopsis*. Therefore, cytokinins have a crucial role in *Marchantia*
289 development, and fine-tuning of the cytokinin signaling involving type-A and type-B RRs is
290 likely an ancestral mechanism controlling plant organ growth. In *Arabidopsis*, six cytokinin
291 response factors (CRFs) function as transcription factors and control cytokinin signaling
292 (Raines et al. 2016). Both RRs and CRFs are regulated by the CHK-HPT phosphorelay,

293 although they work independently (Rashotte et al. 2006). The *Marchantia* genome encodes one
294 CRF (MpCRF, Mapoly0023s0075). Since the *Mprrb* knockout lines displayed severe
295 morphological defects but not lethality, it is probable that cytokinin signaling is mediated by
296 MpCRF as well as MpRRB. Further studies on downstream events regulated by MpRRB and
297 MpCRF will clarify the intrinsic role of cytokinin signaling in growth, development and
298 responses to internal and external cues.

299 We isolated only one MpRRB-overexpressing line from 330 pieces of thallus, and
300 this line exhibited a much severer phenotype than the *Mprra* knockout line (Fig. 5;
301 Supplementary Fig. S5). This suggests that an excess amount of MpRRB has a deleterious
302 effect on *Marchantia* development. By contrast, a previous report demonstrated that
303 overexpression of *ARR1*, one of the type-B RRs in *Arabidopsis*, resulted in subtle phenotypic
304 changes, producing hypertrophic cotyledons, and longer cotyledonary petioles and shorter roots
305 as compared with wild-type (Sakai et al. 2001). However, a combination of *ARR1*
306 overexpression and cytokinin treatment caused disordered cell proliferation in the shoot apex,
307 thereby leading to growth defects (Sakai et al. 2001). This and our results suggest that in
308 *Marchantia*, the endogenous cytokinin level is high enough to activate MpRRB. Indeed,
309 *Marchantia* accumulates a higher level of cytokinins than *Arabidopsis* (Table 1), and only
310 inhibitory effects were observed by treatment with 10 μ M or 50 μ M cytokinins (Supplementary
311 Figs. S1, S2). Flores-Sandoval et al. (2016) also reported that a high dose of BA inhibited
312 *Marchantia* growth.

313 Our cytokinin measurements showed that cZ-type cytokinins were more abundant
314 than the other types in *Marchantia* (Table 1), although tZ- and iP-types are major cytokinin
315 species in *Arabidopsis* (Sakakibara 2006). In another lineage of basal land plants,

316 *Physcomitrella patens*, the most abundant cytokinins are also cZ-types (von Schwartzberg et
317 al. 2007), and the same applies to cyanobacteria and algae (Stirk et al. 2013, Žižková et al.
318 2017). Indeed, tRNA-isopentenyltransferases (IPTs) involved in biosynthesis of cZ-type
319 cytokinins exist in algae, *Marchantia* and *Physcomitrella*, while adenylate-IPTs, which
320 catalyze the first step of biosynthesis of tZ- and iP-types, are missing (Bowman et al. 2017,
321 Yevdakova and von Schwartzberg 2007). This suggests that the major pathways for cytokinin
322 biosynthesis have changed during plant evolution. A previous study showed that a *Marchantia*
323 MpCHK exhibited a lower response to all tested cytokinins including cZ than *Arabidopsis*
324 AHK4 or *Physcomitrella* PpCHK4, although it is unclear which of the two *Marchantia*
325 MpCHKs was used for the bacterial complementation assay (Gruhn et al. 2014). The lower
326 cytokinin response of MpCHK may make *Marchantia* insensitive to exogenously applied
327 cytokinins. Besides, 6-day preculture of gemmae prior to cytokinin treatment may be another
328 reason for the insensitivity, because, in the case of auxin treatment, much milder effects were
329 observed in samples with 6-day preculture than in those without preculture (Ishizaki et al. 2012,
330 Flores-Sandoval et al. 2015). While the dorsiventral polarity is established during the 6-day
331 preculture (Bowman 2016), what kind of physiological events occur remains elusive. It is
332 probable that the permeability of cytokinins changes due to alterations in the components of the
333 cell wall and/or the plasma membrane.

334 Previous studies have demonstrated that in contrast to cytokinins, auxin inhibits
335 gemma cup formation, and enhances rhizoid production and epinastic thallus growth in
336 *Marchantia* (Ishizaki et al. 2012, Flores-Sandoval et al. 2015, Eklund et al. 2015). This suggests
337 that cytokinins and auxin have antagonistic functions in the formation of gemma cups and
338 rhizoid, and in thallus growth. During plant evolution, the phosphorelay system controlling

339 cytokinin and ethylene signaling emerged earlier than F-box-mediated hormone pathways,
340 which are represented by auxin signaling (Bowman et al. 2017). Therefore, it is likely that
341 plants exploited auxin signaling to attenuate the cytokinin-mediated pathway in order to
342 regulate organ formation under changing environmental conditions on land. In *Marchantia*,
343 gemma cups and rhizoids are produced very close to the apical cell, and cell fate is determined
344 within a few cell divisions (Shimamura 2016), suggesting that cytokinins and auxin exert their
345 antagonistic functions in the early descendants of stem cells. Further studies will reveal how
346 the two hormones communicate with each other during the initial process of organ formation.

347

348 **Materials and Methods**

349 **Plant materials and growth conditions**

350 The male and female *Marchantia* accessions Takaragaike (Tak)-1 and Tak-2, respectively,
351 were cultured on half-strength Gamborg's B5 agar medium under continuous white light at
352 22°C. F1 spores were obtained by crossing Tak-1 and Tak-2. For formation of sexual organs,
353 mature thalli were cultured under white light supplemented with far-red light (Ishizaki et al.
354 2016).

355

356 **Cloning of MpRRs and MpCKX2**

357 MpRR cDNAs were amplified by RT-PCR using total RNA prepared from Tak-1 thalli and the
358 primers listed in Supplementary Table S1, and were then cloned into the plasmid pDONR221
359 using BP Clonase (Thermo Fisher Scientific, USA) to obtain a Gateway entry clone. MpCKX2
360 cDNA was amplified by RT-PCR using total RNA prepared from Tak-1 thalli and the primers

361 listed in Supplementary Table S1, followed by cloning into the plasmid pENTR/D-TOPO
362 (Thermo Fisher Scientific) to obtain a Gateway entry clone.

363

364 **Quantification of cytokinins**

365 Wild-type (Tak-1) gemmae were grown for one- or three-weeks on half-strength Gamborg's
366 B5 agar medium. For three-week-old thallus, the apical part (0-3 mm from the tip) and the basal
367 part (3-10 mm from the tip) were separately collected. Approximately 100 mg of each sample
368 was subjected to cytokinin measurement by ultra-performance liquid chromatography (UPLC)-
369 tandem mass spectrometry (AQUITY UPLC System/XEVO-TQS; Waters, USA) with an ODS
370 column (AQUITY UPLC HSS T3, 1.8 μm , 2.1 \times 100 mm; Waters) as previously described
371 (Kojima et al. 2009).

372

373 **Generation of overexpression and knockout lines**

374 To obtain overexpression lines of *MpRRA* and *MpRRB*, each cDNA in pDONR221 was
375 transferred to the destination vector pMpGWB103 (Ishizaki et al. 2015) by LR Clonase
376 (Thermo Fisher Scientific) to be fused with the *MpEFI α* promoter. The resultant plasmids were
377 used for transformation of Tak-1 as described by Kubota et al. (2013).

378 To obtain knockout lines of *MpRRA* and *MpRRB*, the 5'- and 3'-homologous arms
379 were amplified from Tak-1 genomic DNA by PCR using the primers listed in Supplementary
380 Table S1. The amplified 5'- and 3'-fragments were cloned into the *PacI* and *AscI* sites,
381 respectively, of the pJHY-TMp1 vector (Ishizaki et al. 2013) with an In-Fusion HD cloning kit
382 (Takara Bio, Japan). The plasmid was used for transformation of F1 sporelings (Ishizaki et al.
383 2008). Knockout lines were identified as described previously (Ishizaki et al. 2013). To conduct

384 complementation tests of *Mprrr* knockout lines, the promoter and coding sequences of *MpRRs*
385 were amplified from Tak-1 genomic DNA by PCR using the primers listed in Supplementary
386 Table S1. The amplified fragments were cloned into pDONR221, followed by an LR reaction
387 to transfer them to the destination vector pMpGWB301 (Ishizaki et al. 2015).

388

389 **GUS expression analysis**

390 The 5-kb genomic regions immediately upstream of the start codon of *MpRRs* were amplified
391 by PCR using Tak-1 genomic DNA and the primers listed in Supplementary Table S1. The
392 amplified fragments were cloned into pDONR221, followed by an LR reaction to transfer them
393 to the destination vector pMpGWB104 (Ishizaki et al. 2015), generating a fusion to the *GUS*
394 gene. After transformation of Tak-1 and Tak-2, hygromycin-resistant plantlets were selected to
395 establish isogenic lines. GUS staining was performed as described by Althoff et al. (2014).

396

397 **RT-PCR**

398 To quantify the *MpRRA* transcript level, thallus tips were incubated in half-strength Gamborg's
399 B5 liquid medium for 24 h with shaking at 130 rpm, and then tZ was added to the medium to a
400 final concentration of 50 μ M, followed by a further 2-h incubation. Total RNA was extracted
401 with a FavorPrep Plant Total RNA Purification Mini Kit (Favorgen Biotech, Taiwan). First-
402 strand cDNAs were prepared from total RNA with ReverTra Ace qPCR RT Master Mix with
403 gDNA Remover (TOYOBO, Japan) according to the manufacturer's instruction. Semi-
404 quantitative RT-PCR was conducted with a Gene Amp PCR System (Thermo Fisher Scientific).
405 qRT-PCR was performed with a THUNDERBIRD SYBR qPCR Mix (TOYOBO) and the

406 LightCycler 480 Real-Time PCR System (Roche, Switzerland). The primers used for RT-PCR
407 are listed in Supplementary Table S1.

408

409 **3D imaging of the apical notch**

410 Ten-day-old thalli were fixed with 4% paraformaldehyde in PBS under vacuum for 2 h. Fixed
411 samples were washed twice with PBS and transferred to ClearSee solution (10% xylitol, 15%
412 sodium deoxycholate and 25% urea) (Kurihara et al. 2015). The cell wall was stained overnight
413 with 0.1% DirectRed23 (Sigma-Aldrich, USA) in ClearSee solution. Stained samples were
414 washed with ClearSee solution for more than an hour, and observed under a confocal laser
415 scanning microscope (Zeiss LSM880). DirectRed23 was excited at 543 nm. 3D images were
416 reconstructed from multiple images of horizontal sections.

417

418 **Funding**

419 This work was supported by MEXT KAKENHI (17H06470 and 17H06477 to M.U., 18H04836
420 to R.N., 17H06472 to K.I.) and JSPS KAKENHI (17H03965 to M.U., 16K07398 to R.N.).

421

422 **Disclosures**

423 The authors declare no conflicts of interest associated with this manuscript.

424

425 **Acknowledgements**

426 We thank Dr. Makoto Hayashi and Dr. Takatoshi Kiba for helpful discussions, and Ms. Sakiko
427 Ishida for technical assistance.

428

429 **References**

- 430 Althoff, F., Kopischke, S., Zobell, O., Ide, K., Ishizaki, K., Kohchi, T., et al. (2014)
431 Comparison of the *MpEF1a* and *CaMV35* promoters for application in *Marchantia*
432 *polymorpha* overexpression studies. *Transgenic Res.* 23: 235–244.
- 433 Argyros, R.D., Mathews, D.E., Chiang, Y.H., Palmer, C.M., Thibault, D.M., Etheridge, N., et
434 al. (2008) Type B response regulators of *Arabidopsis* play key roles in cytokinin signaling
435 and plant development. *Plant Cell* 20: 2102–2116.
- 436 Barnes, C.R. and Land, W.J.G. (1908) The origin of the cupule of *Marchantia*. *Bot. Gaz.* 46:
437 401-409.
- 438 Bowman, J.L. (2016) A brief history of *Marchantia* from Greece to genomics. *Plant Cell*
439 *Physiol.* 57: 210–229.
- 440 Bowman, J.L., Kohchi, T., Yamato, K.T., Jenkins, J., Shu, S., Ishizaki, K., et al. (2017) Insights
441 into land plant evolution garnered from the *Marchantia polymorpha* genome. *Cell* 171: 287–
442 304. e15.
- 443 Brenner, W.G., Romanov, G.A., Kollmer, I., Burkle, L. and Schmülling, T. (2005) Immediate-
444 early and delayed cytokinin response genes of *Arabidopsis thaliana* identified by genome-
445 wide expression profiling reveal novel cytokinin-sensitive processes and suggest cytokinin
446 action through transcriptional cascades. *Plant J.* 44: 314–333.
- 447 Choi, S.H., Hyeon, D.Y., Lee, I.H., Park, S.J., Han, S., Lee, I.C., et al. (2014) Gene duplication
448 of type-B ARR transcription factors systematically extends transcriptional regulatory
449 structures in *Arabidopsis*. *Sci. Rep.* 4: 7197–7205.

450 Dello Ioio, R., Nakamura, K., Moubayidin, L., Perilli, S., Taniguchi, M., Morita, M.T., et al.
451 (2008) A genetic framework for the control of cell division and differentiation in the root
452 meristem. *Science* 322: 1380–1384.

453 Eklund, D.M., Ishizaki, K., Flores-Sandoval, E., Kikuchi, S., Takebayashi, Y., Tsukamoto, S.,
454 et al. (2015) Auxin produced by the indole-3-pyruvic acid pathway regulates development
455 and gemmae dormancy in the liverwort *Marchantia polymorpha*. *Plant Cell* 27: 1650-1669.

456 Flores-Sandoval, E., Eklund, D.M. and Bowman, J.L. (2015) A Simple auxin transcriptional
457 response system regulates multiple morphogenetic processes in the liverwort *Marchantia*
458 *polymorpha*. *PLoS Genet.* 28: e1005207

459 Flores-Sandoval, E., Dierschke, T., Fisher, T.J. and Bowman, J.L. (2016) Efficient and
460 inducible use of artificial microRNAs in *Marchantia polymorpha*. *Plant Cell Physiol.* 57:
461 281–290.

462 Gruhn, N., Halawa, M., Snel, B., Seidl, M.F. and Heyl, A. (2014) A subfamily of putative
463 cytokinin receptors is revealed by an analysis of the evolution of the two-component
464 signaling system of plants. *Plant Physiol.* 165: 227-237.

465 Hwang, I. and Sheen, J. (2001) Two-component circuitry in *Arabidopsis* cytokinin signal
466 transduction. *Nature* 413: 383–389.

467 Ishida, K., Yamashino, T., Yokoyama, A. and Mizuno, T. (2008) Three type-B response
468 regulators, ARR1, ARR10 and ARR12, play essential but redundant roles in cytokinin signal
469 transduction throughout the life cycle of *Arabidopsis thaliana*. *Plant Cell Physiol.* 49: 47–
470 57.

471 Ishizaki, K., Chiyoda, S., Yamato, K.T. and Kohchi, T. (2008) *Agrobacterium*-mediated
472 transformation of the haploid liverwort *Marchantia polymorpha* L., an emerging model for
473 plant biology. *Plant Cell Physiol.* 49: 1084-1091.

474 Ishizaki, K., Nonomura, M., Kato, H., Yamato, K.T. and Kohchi, T. (2012) Visualization of
475 auxin-mediated transcriptional activation using a common auxin-responsive reporter system
476 in the liverwort *Marchantia polymorpha*. *J. Plant Res.* 125: 643–651.

477 Ishizaki, K., Johzuka-Hisatomi, Y., Ishida, S., Iida, S. and Kohchi, T. (2013) Homologous
478 recombination-mediated gene targeting in the liverwort *Marchantia polymorpha* L. *Sci. Rep.*
479 3: 1532.

480 Ishizaki, K., Nishihama, R., Ueda, M., Inoue, K., Ishida, S., Nishimura, Y., et al. (2015)
481 Development of gateway binary vector series with four different selection markers for the
482 liverwort *Marchantia polymorpha*. *PLoS One* 10: e0138876.

483 Ishizaki, K., Nishihama, R., Yamato, K.T. and Kohchi, T. (2016) Molecular Genetic Tools and
484 Techniques for *Marchantia polymorpha* Research. *Plant Cell Physiol.* 57: 262-270.

485 Kato, H., Ishizaki, K., Kouno, M., Shirakawa, M., Bowman, J.L., Nishihama, R., et al. (2015)
486 Auxin-mediated transcriptional system with a minimal set of components is critical for
487 morphogenesis through the life cycle in *Marchantia polymorpha*. *PLoS Genet.* 11: e1005084.

488 Kieber, J.J. and Schaller, G.E. (2014) Cytokinins. *Arabidopsis Book* 12: e0168.

489 Kim, H.J., Ryu, H., Hong, S.H., Woo, H.R., Lim, P.O., Lee, I.C., et al. (2006) Cytokinin-
490 mediated control of leaf longevity by AHK3 through phosphorylation of ARR2 in
491 *Arabidopsis*. *Proc. Natl. Acad. Sci. USA* 103: 814–819.

492 Ko, D., Kang, J., Kiba, T., Park, J., Kojima, M., Do, J., et al. (2014) *Arabidopsis* ABCG14 is
493 essential for the root-to-shoot translocation of cytokinin. *Proc. Natl. Acad. Sci. USA* 111:
494 7150-7155.

495 Kojima, M., Kamada-Nobusada, T., Komatsu, H., Takei, K., Kuroha, T., Mizutani, M., et al.
496 (2009) Highly sensitive and high-throughput analysis of plant hormones using MS-probe
497 modification and liquid chromatography–tandem mass spectrometry: an application for
498 hormone profiling in *Oryza sativa*. *Plant Cell Physiol.* 50: 1201-1214.

499 Kubota, A., Ishizaki, K., Hosaka, M. and Kohchi, T. (2013) Efficient *Agrobacterium*-mediated
500 transformation of the liverwort *Marchantia polymorpha* using regenerating thalli. *Biosci.*
501 *Biotechnol. Biochem.* 77: 167–172.

502 Kurihara, D., Mizuta, Y., Sato, Y. and Higashiyama, T. (2015) ClearSee: a rapid optical
503 clearing reagent for whole-plant fluorescence imaging. *Development* 142: 4168–4179.

504 Mason, M.G., Mathews, D.E., Argyros, D.A., Maxwell, B.B., Kieber, J.J., Alonso, J.M. et al.
505 (2005) Multiple type-B response regulators mediate cytokinin signal transduction in
506 *Arabidopsis*. *Plant Cell* 17: 3007–3018.

507 Raines, T., Shanks, C., Cheng, C.Y., McPherson, D., Argueso, C.T., Kim, H.J., et al. (2016)
508 The cytokinin response factors modulate root and shoot growth and promote leaf senescence
509 in *Arabidopsis*. *Plant J.* 85: 134–147.

510 Rashotte, A.M., Mason, M.G., Hutchison, C.E., Ferreira, F.J., Schaller, G.E. and Kieber, J.J.
511 (2006) A subset of *Arabidopsis* AP2 transcription factors mediates cytokinin responses in
512 concert with a two-component pathway. *Proc. Natl. Acad. Sci. USA* 103: 11081–11085.

513 Riou-Khamlichi, C., Huntley, R., Jacquard, A. and Murray, J.A. (1999) Cytokinin activation
514 of *Arabidopsis* cell division through a D-type cyclin. *Science* 283: 1541-1544.

515 Sakai, H., Honma, T., Aoyama, T., Sato, S., Kato, T., Tabata, S., et al. (2001) ARR1, a
516 transcription factor for genes immediately responsive to cytokinins. *Science* 294: 1519–1521.

517 Sakakibara, H. (2006) Cytokinins: activity, biosynthesis, and translocation. *Annu. Rev. Plant*
518 *Biol.* 57: 431-449.

519 Schmölling, T., Werner, T., Riefler, M., Krupkova, E., Bartrina, Y. and Manns, I. (2003)
520 Structure and function of cytokinin oxidase/dehydrogenase genes of maize, rice, *Arabidopsis*
521 and other species. *J. Plant Res.* 116: 241–252.

522 Shimamura, M. (2016) *Marchantia polymorpha*: Taxonomy, Phylogeny and Morphology of a
523 Model System. *Plant Cell Physiol.* 57: 230–256.

524 Soni, R., Carmichael, J.P., Shah, Z.H. and Murray, J.A.H. (1995) A family of cyclin D
525 homologs from plants differentially controlled by growth regulators and containing the
526 conserved retinoblastoma protein interaction motif. *Plant Cell* 7: 85-103.

527 Stirk, W.A., Ördög, V., Novák, O., Rolčik, J., Strnad, M., Bálint, P., et al. (2013) Auxin and
528 cytokinin relationships in twenty-four microalgae strains. *J. Phycol.* 49: 459-467.

529 Suzuki, T., Imamura, A., Ueguchi, C. and Mizuno, T. (1998) Histidine-containing
530 phosphotransfer (HPT) signal transducers implicated in His-to-Asp phosphorelay in
531 *Arabidopsis*. *Plant Cell Physiol.* 39: 1258-1268.

532 Taniguchi, M., Sasaki, N., Tsuge, T., Aoyama, T. and Oka, A. (2007) ARR1 directly activates
533 cytokinin response genes that encode proteins with diverse regulatory functions. *Plant Cell*
534 *Physiol.* 48: 263–277.

535 To, J.P.C., Haberer, G., Ferreira, F.J., Deruère, J., Mason, M.G., Schaller, G.E., et al. (2004)
536 Type-A *Arabidopsis* response regulators are partially redundant negative regulators of
537 cytokinin signaling. *Plant Cell* 16: 658-671.

538 To, J.P.C., Deruère, J., Maxwell, B.B., Morris, V.F., Hutchison, C.E., Ferreira, F.J., et al. (2007)
539 Cytokinin regulates type-A *Arabidopsis* response regulator activity and protein stability via
540 two-component phosphorelay. *Plant Cell* 19: 3901–3914.

541 von Schwartzberg, K., Núñez, M.F., Blaschke, H., Dobrev, P.I., Novák, O., Motyka, V., et
542 al. (2007) Cytokinins in the bryophyte *Physcomitrella patens*: analyses of activity,
543 distribution, and cytokinin oxidase/dehydrogenase overexpression reveal the role of
544 extracellular cytokinins. *Plant Physiol.* 145: 786-800.

545 Wang, Y.H. and Irving, H.R. (2011) Developing a model of plant hormone interactions. *Plant*
546 *Signal. Behav.* 6: 494-500.

547 Yevdakova, N.A. and von Schwartzberg, K. (2007) Characterisation of a prokaryote-type
548 tRNA-isopentenyltransferase gene from the moss *Physcomitrella patens*. *Planta* 226: 683–
549 695.

550 Žižková, E., Kubeš, M., Dobrev, P.I., Příbyl, P., Šimura, J., Zahajská, L., et al. (2017) Control
551 of cytokinin and auxin homeostasis in cyanobacteria and algae. *Ann. Bot.* 119: 151-166.

Table 1. Quantification of cytokinins.										
Hormone		One-week-old thallus (pmol/g fresh weight)			Three-week-old thallus (pmol/g fresh weight)					
					Apical part			Basal part		
		Tak-1	MpCKX2 ^{#7}	MpCKX2 ^{#9}	Tak-1	MpCKX2 ^{#7}	MpCKX2 ^{#9}	Tak-1	MpCKX2 ^{#7}	MpCKX2 ^{#9}
tZ-type	tZ	1.29 ± 0.28	u.q.	u.q.	0.08 ± 0.03	u.q.	u.q.	0.13 ± 0.03	u.q.	u.q.
	tZR	0.05 ± 0.02	0.03 ± 0.01	0.04 ± 0.00	u.q.	u.q.	u.q.	u.q.	0.02	0.02 ± 0.00
	tZRP s	17.53 ± 1.61	8.54 ± 1.20	8.29 ± 1.38	4.98 ± 1.21	2.36 ± 1.07	2.50 ± 0.36	3.67 ± 0.87	1.46 ± 0.30	0.92 ± 0.18
	tZ7G	u.q.	u.q.	u.q.	u.q.	u.q.	u.q.	u.q.	u.q.	u.q.
	tZ9G	u.q.	u.q.	u.q.	u.q.	u.q.	u.q.	u.q.	u.q.	u.q.
	tZOG	0.23 ± 0.09	u.q.	u.q.	u.q.	u.q.	u.q.	0.17 ± 0.10	u.q.	u.q.
	tZROG	u.q.	u.q.	u.q.	u.q.	u.q.	u.q.	u.q.	u.q.	u.q.
	tZRPsOG	u.q.	u.q.	u.q.	u.q.	u.q.	u.q.	u.q.	u.q.	u.q.
cZ-type	cZ	3.82 ± 0.29	0.10 ± 0.03	0.20 ± 0.03	2.91 ± 0.91	0.08 ± 0.02	0.22 ± 0.04	1.50 ± 0.28	0.18 ± 0.15	0.34 ± 0.07
	cZR	0.20 ± 0.06	0.23 ± 0.05	0.42 ± 0.13	0.56 ± 0.18	0.23 ± 0.12	0.44 ± 0.13	0.17 ± 0.05	0.58 ± 0.05	1.11 ± 0.55
	cZRP s	66.69 ± 9.28	52.76 ± 7.80	74.39 ± 9.09	114.85 ± 9.93	58.84 ± 2.57	77.89 ± 13.42	35.39 ± 9.42	33.86 ± 4.99	34.46 ± 3.00
	cZOG	2.98 ± 0.28	0.14	u.q.	1.48 ± 0.31	u.q.	0.11	5.13 ± 2.08	0.57 ± 0.09	0.27 ± 0.05
	cZROG	0.16 ± 0.03	0.13 ± 0.02	0.19 ± 0.04	0.49 ± 0.05	0.59 ± 0.06	0.99 ± 0.05	0.21 ± 0.05	0.49 ± 0.07	0.57 ± 0.06
	cZRPsOG	u.q.	u.q.	u.q.	0.11 ± 0.01	0.06	0.06 ± 0.01	u.q.	0.04	0.03
DZ-type	DZ	u.q.	u.q.	u.q.	u.q.	u.q.	u.q.	u.q.	u.q.	u.q.
	DZR	u.q.	u.q.	u.q.	u.q.	u.q.	u.q.	u.q.	u.q.	u.q.
	DZRP s	u.q.	u.q.	u.q.	u.q.	u.q.	u.q.	u.q.	u.q.	u.q.
	DZ9G	u.q.	u.q.	u.q.	u.q.	u.q.	u.q.	u.q.	u.q.	u.q.
iP-type	iP	0.51 ± 0.02	u.q.	0.10 ± 0.03	0.58 ± 0.05	u.q.	0.12 ± 0.03	0.22 ± 0.02	0.35	0.07 ± 0.02
	iPR	0.040	u.q.	0.06 ± 0.04	0.13 ± 0.03	u.q.	0.08 ± 0.02	0.06 ± 0.01	u.q.	0.27 ± 0.15
	iPRP s	21.78 ± 4.13	15.58 ± 2.57	29.93 ± 3.31	41.59 ± 3.07	13.24 ± 4.81	46.36 ± 5.15	15.33 ± 2.92	12.13 ± 0.30	27.25 ± 2.90
	iP7G	u.q.	u.q.	u.q.	u.q.	u.q.	u.q.	u.q.	u.q.	u.q.
	iP9G	u.q.	u.q.	u.q.	u.q.	u.q.	u.q.	u.q.	u.q.	u.q.

Amounts of cytokinins were measured in 1- and 3-week-old thalli of wild-type (Tak-1) and MpCKX2-overexpressing lines #7 and #9. For 3-week-old thallus, cytokinin content in apical and basal parts was separately measured. Data are presented as mean ± SD (n ≥ 3). u.q., under quantification limit.

552

553

554 **Figure Legends**

555 **Fig. 1** Overexpression of MpCKX2. (A) Expression levels of MpCKX2. qRT-PCR was
556 conducted using total RNA from MpCKX2-overexpressing lines #7 and #9. mRNA levels were
557 normalized to that of MpEF1 α . Data are presented as mean \pm SD (n = 3). Significant differences
558 from wild-type (Tak-1) were determined by Student's *t*-test: **, *P* < 0.01. (B) Thalli and
559 rhizoids of MpCKX2-overexpressing lines. Gemmae were cultured for 21 days. Bars represent
560 5 mm. (C, D) Thallus area (C) and gemma cup number per thallus area (D) of MpCKX2-
561 overexpressing lines. Data are presented as mean \pm SD (n = 20). Significant differences from
562 wild-type were determined by Student's *t*-test: **, *P* < 0.01. (E) Vertical longitudinal optical
563 sections of the apical notch in 10-day-old thalli of wild-type (Tak-1) and MpCKX2-
564 overexpressing lines. Gemmiparous cells in the initial stage (wild-type, left) and the subsequent
565 growth stage (wild-type, right) are shown in orange color. An elongated gemmiparous cell
566 observed in the growth stage is indicated by a white arrowhead. Asterisks indicate apical or
567 sub-apical cells. Note that no gemmiparous area is visible in the sections of MpCKX2-
568 overexpressing lines #7 and #9. Bars represent 50 μ m.

569

570 **Fig. 2** Protein structures of cytokinin signaling components in *Marchantia*. (A, B) Protein
571 structures of type-A RRs (A) and type-B RRs (B). The receiver domains (gray boxes), GARP
572 domains (black boxes) and glutamine- and proline-rich regions (Q/P-rich) are shown. Three
573 phosphorylation sites in the receiver domain are indicated as D-D-K. The percentage of amino
574 acid identities between the pairs of sequences is shown. (C) Protein structures of CHKs. The
575 CHASE domain, histidine kinase domain (HK), receiver-like domain (RL) and receiver domain

576 (R) are shown. (D) Protein structures of HPTs. The HPT domain is shown. The percentage
577 amino acid identity between pairs of sequences is indicated.

578

579 **Fig. 3** Expression patterns of MpRRs. (A, B) Expression levels of MpRRA (A) and MpRRB (B).
580 qRT-PCR was conducted using total RNA from 1-week-old (young) and 3-week-old (mature)
581 thalli, and antheridiophores and archegoniophores. mRNA levels were normalized to that of
582 MpEF1 α . Data are presented as mean \pm SD (n = 3). (C-V) GUS staining of
583 *proMpRRA:MpRRA-GUS* (C-L) and *proMpRRB:MpRRB-GUS* (M-V). Gemmae (C, M), 5-
584 day-old thallus (D), 7-day-old thallus (N), 10-day-old thallus (E, O), the tip region of 10-day-
585 old thallus (F, P), 20-day-old thallus (G, Q), transverse section of a gemma cup on 20-day-old
586 thallus (H, R), young antheridiophore (I, S), mature antheridiophore (J, T), young
587 archegoniophore (K, U), and mature archegoniophore (L, V). The insets in (D) and (N) are
588 enlarged images of the notch region. Arrowheads indicate apical notches. Bars represent 500
589 μ m.

590

591 **Fig. 4** Phenotype of *Mprrb* knockout lines. (A) Schematic representation of the MpRRB locus.
592 Exons are represented by black boxes. The hygromycin phosphotransferase gene (*hpt*) was
593 inserted into the receiver domain by homologous recombination. (B) MpRRB expression in an
594 *Mprrb* knockout line and two complementation lines. Expression levels were measured by
595 semi-quantitative RT-PCR using total RNA from the knockout line #307 and the
596 complementation lines #10 and #12. MpEF1 α was used as a control. (C) Thalli and rhizoids of
597 the *Mprrb* knockout line and the complementation lines (*Mprrb*^{ko} Comp). The pieces of thallus
598 tip were cultured for 15 days. Bars represent 5 mm. (D) Gemma cup number per thallus area.

599 Data are presented as mean \pm SD (n = 20). Significant differences from wild-type (Tak-2) were
600 determined by Student's *t*-test: **, $P < 0.01$.

601

602 **Fig. 5** Phenotype of *Mprra* knockout lines. (A) Schematic representation of the *MpRRA* locus.
603 Exons are represented by black boxes. The hygromycin phosphotransferase gene (*hpt*) was
604 inserted into the receiver domain by homologous recombination. (B) *MpRRA* expression in
605 *Mprra* knockout line and complementation lines (*Mprra*^{ko} Comp). Expression levels were
606 measured by semi-quantitative RT-PCR using total RNA from the knockout line #289 and the
607 complementation lines #10 and #13. *MpEFI α* was used as a control. (C) Thalli and rhizoids of
608 the *Mprra* knockout line and the complementation lines. The pieces of thallus tip were cultured
609 for 15 days. Bars represent 5 mm. (D) Gemma cup number per thallus area. Data are presented
610 as mean \pm SD (n = 20). Significant differences from wild-type (Tak-2) were determined by
611 Student's *t*-test: **, $P < 0.01$.

612

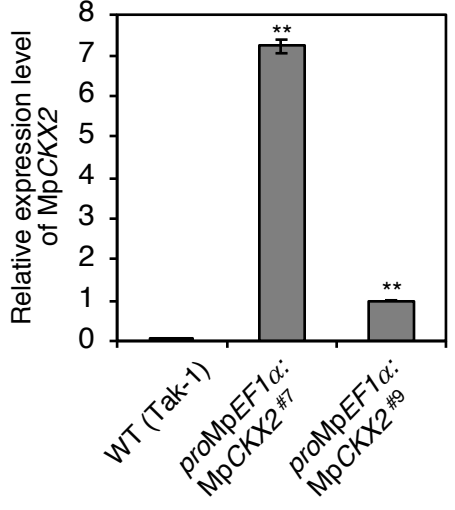
613 **Fig. 6** Phenotype of *MpRRA*-overexpressing lines. (A) *MpRRA* expression in *MpRRA*-
614 overexpressing lines. qRT-PCR was conducted using total RNA from lines #1 and #4. mRNA
615 levels were normalized to that of *MpEFI α* . Data are presented as mean \pm SD (n = 3). Significant
616 differences from wild-type (Tak-1) were determined by Student's *t*-test: **, $P < 0.01$. (B) Thalli
617 and rhizoids of the *MpRRA*-overexpressing lines. The pieces of thallus tip were cultured for 15
618 days. Bars represent 5 mm. (C) Gemma cup number per thallus area. Data are presented as
619 mean \pm SD (n = 20). Significant differences from wild-type (Tak-1) were determined by
620 Student's *t*-test: **, $P < 0.01$.

621

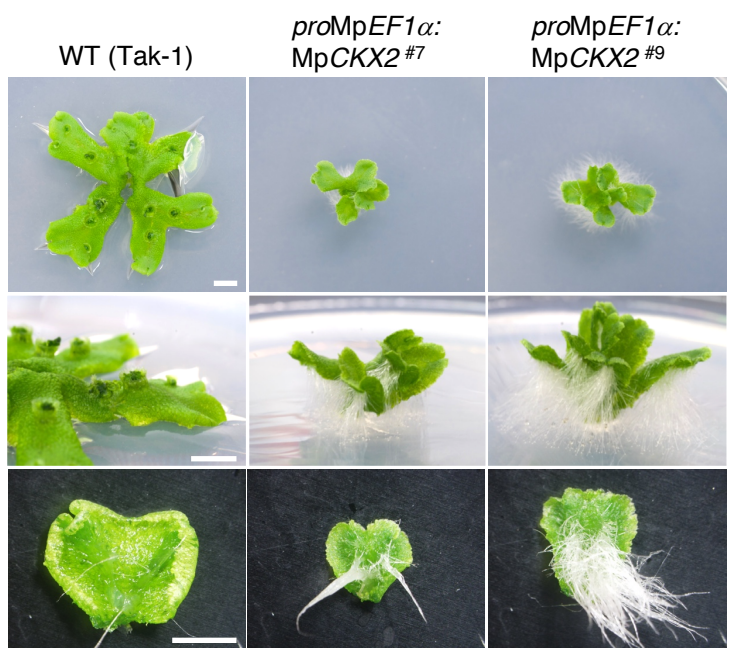
622 **Fig. 7** *MpRRA* expression in transgenic lines. (A) Transcript levels of *MpRRA* in the *MpCKX2*-
623 overexpressing lines. (B) Transcript levels of *MpRRA* in the *Mprrb* knockout line #307 with or
624 without 50 μ M tZ treatment. (C) Transcript levels of *MpRRA* in the *MpRRB*-overexpressing
625 line #15. mRNA levels were normalized to that of *MpEF1 α* . Data are presented as mean \pm SD
626 (n = 3). Significant differences from wild-type (A, C) or the samples with mock treatment (B)
627 were determined by Student's *t*-test: **P* < 0.05, ** *P* < 0.01.

Fig. 1

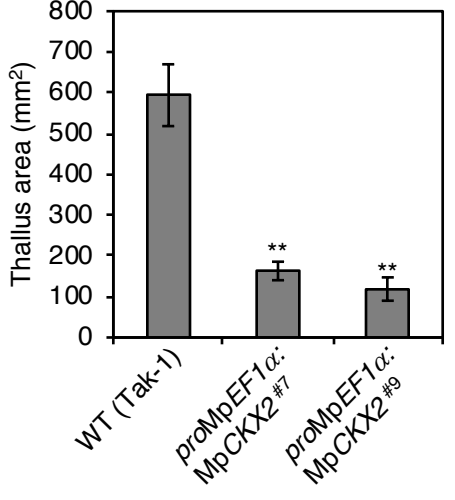
A



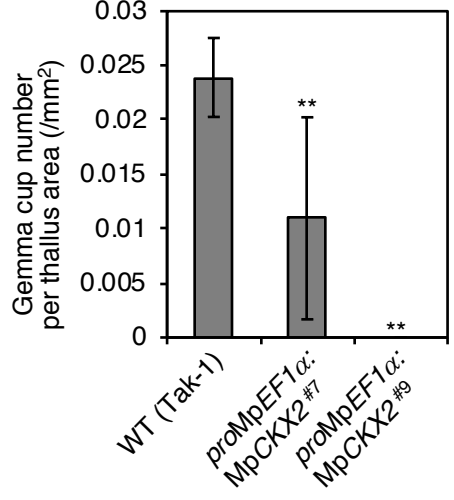
B



C



D



E

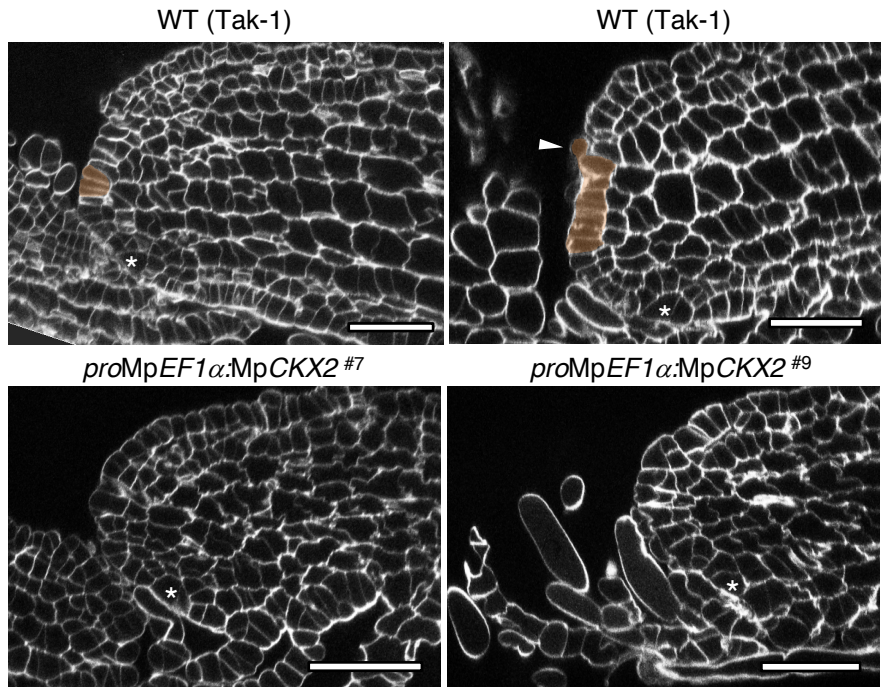
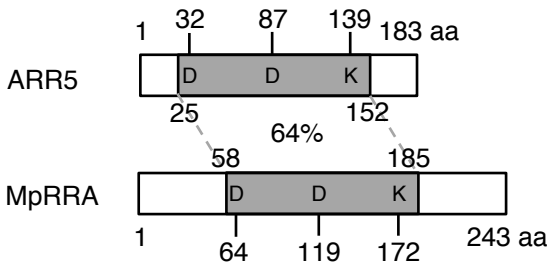


Fig. 2

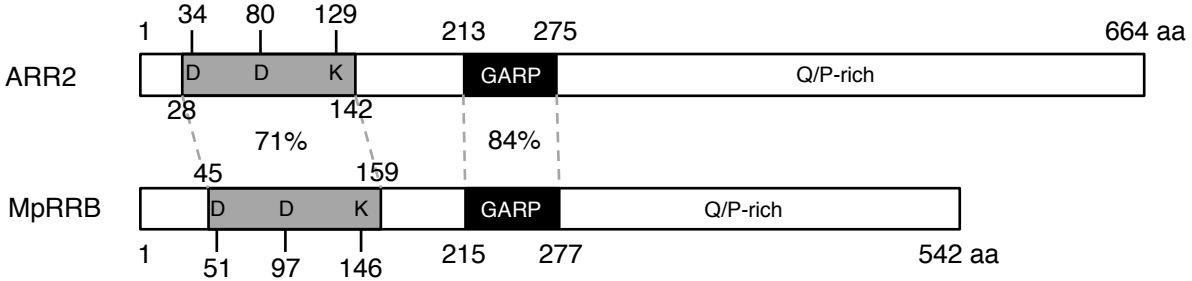
A

Type-A RR

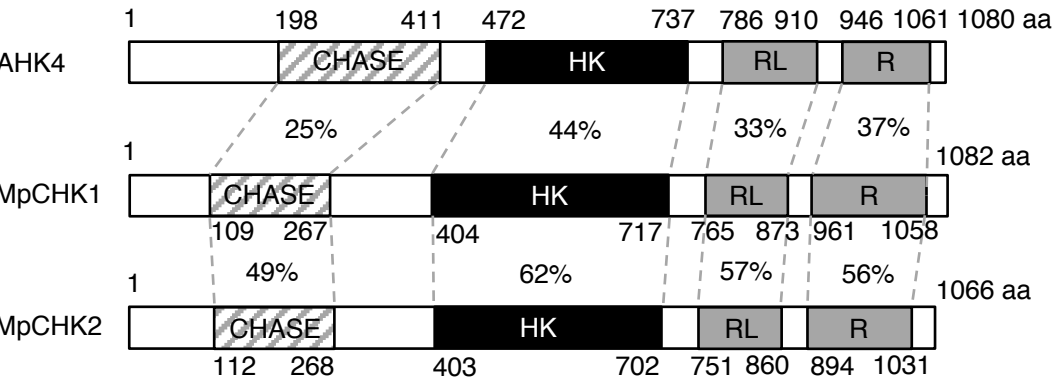


B

Type-B RR



C



D

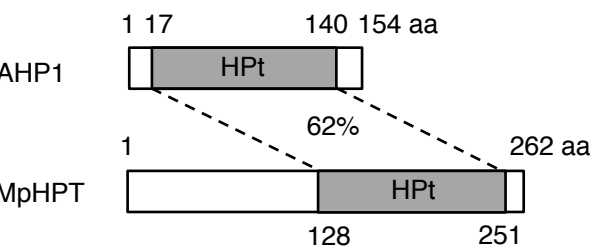
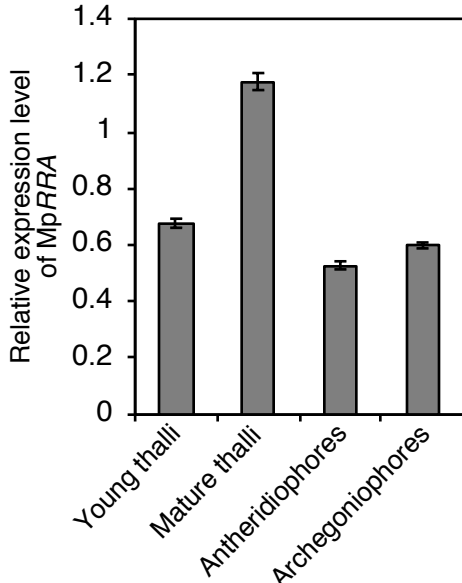
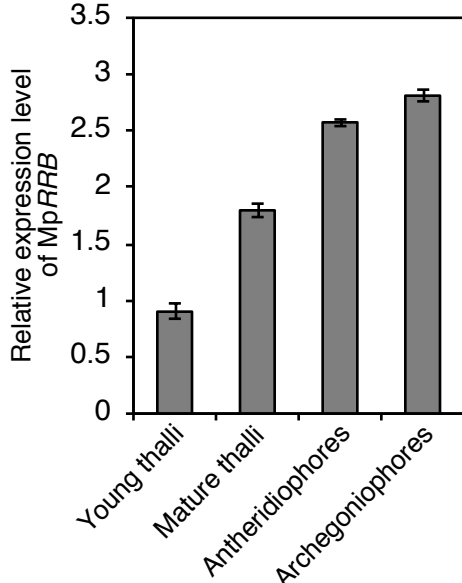


Fig. 3

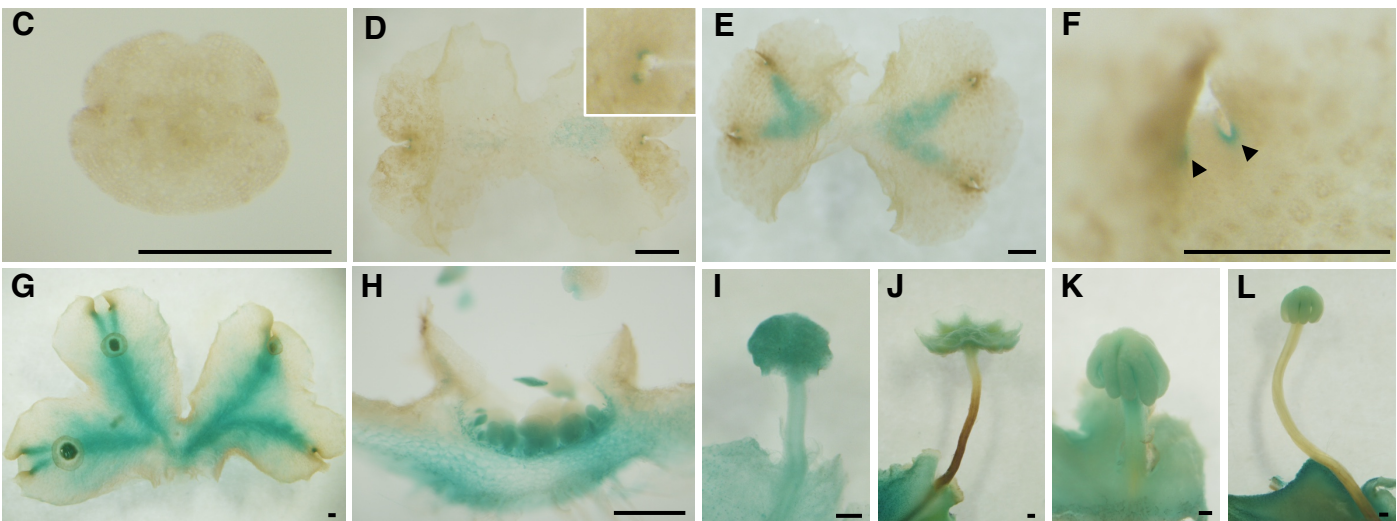
A



B



proMpRRA:GUS



proMpRRB:GUS

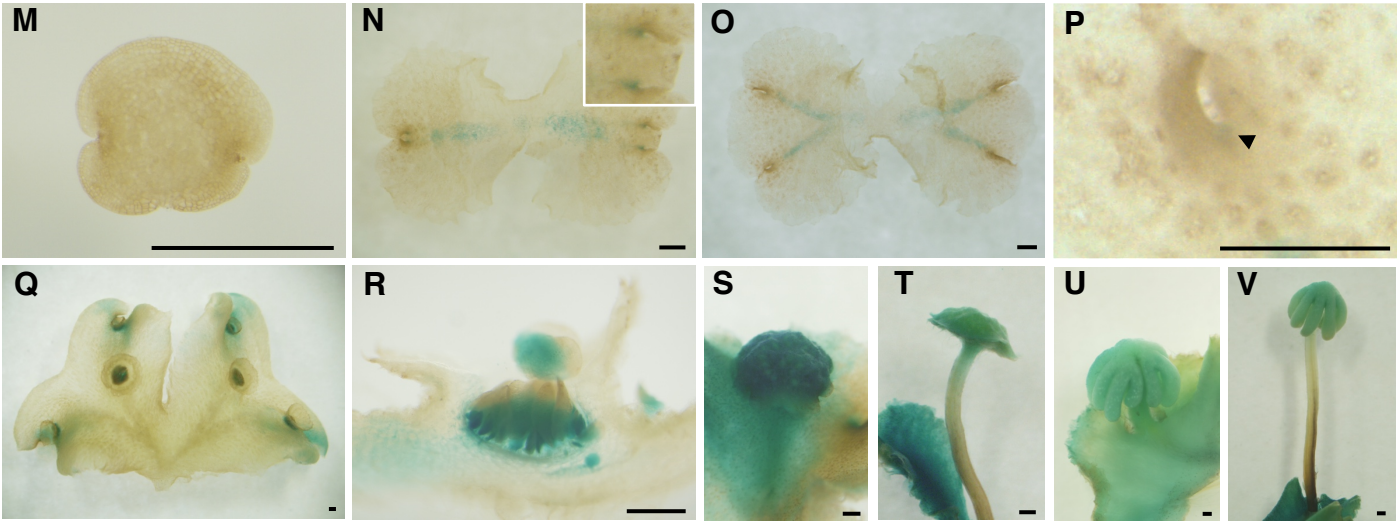
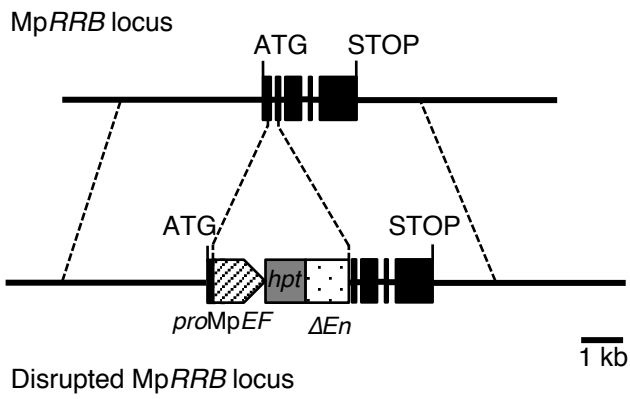
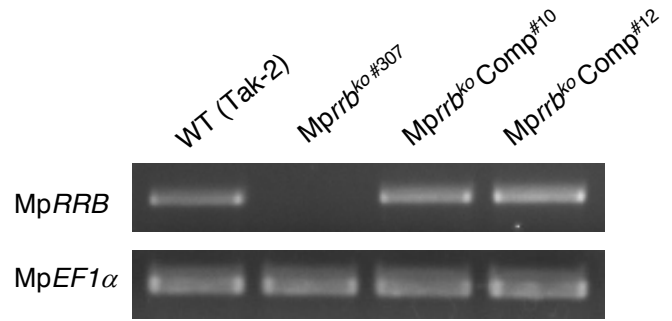


Fig. 4

A



B



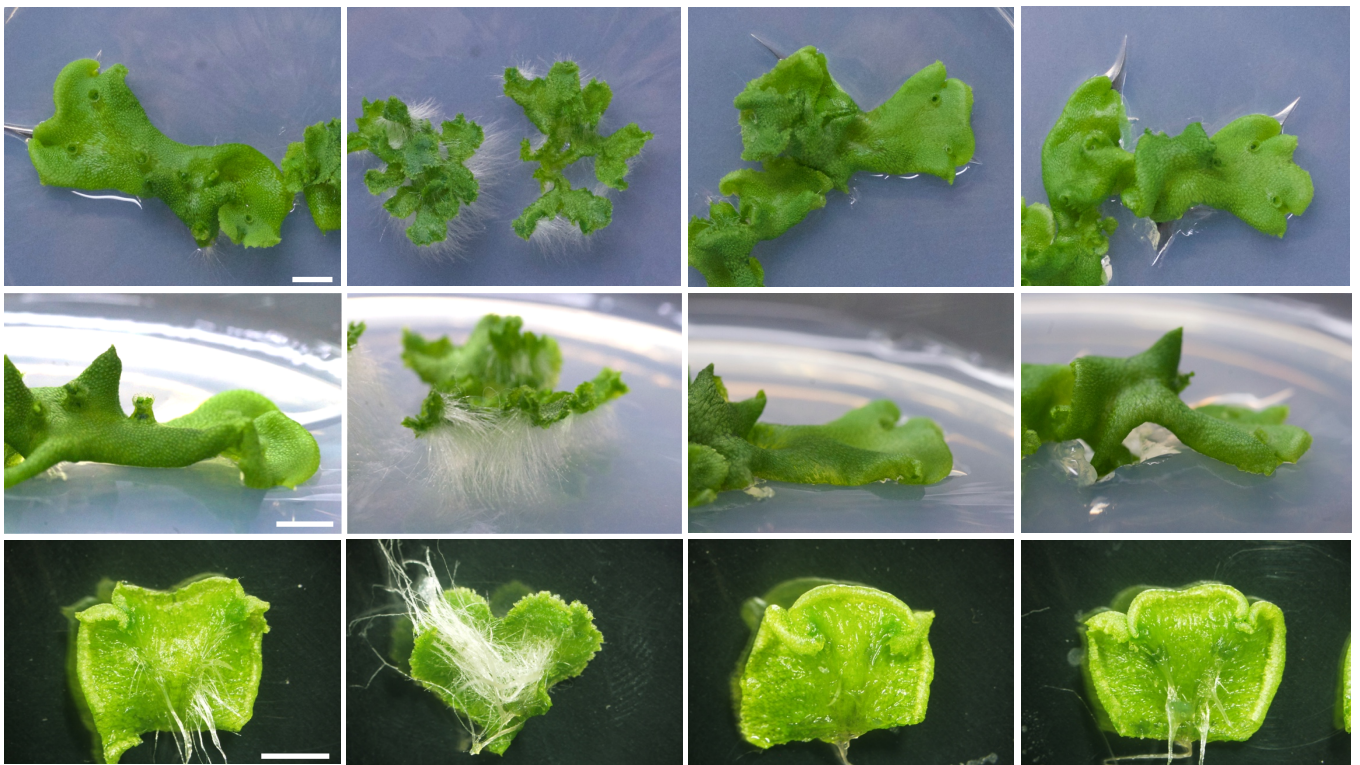
C

WT (Tak-2)

Mprrb^{ko} #307

Mprrb^{ko} Comp#10

Mprrb^{ko} Comp#12



D

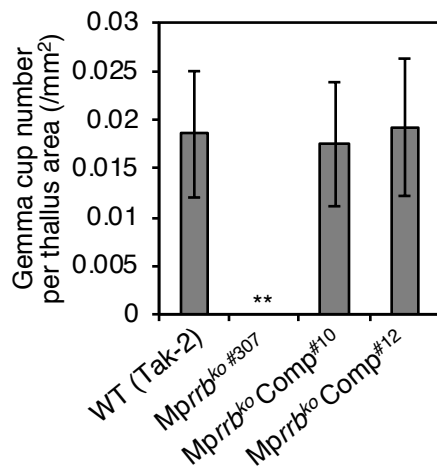
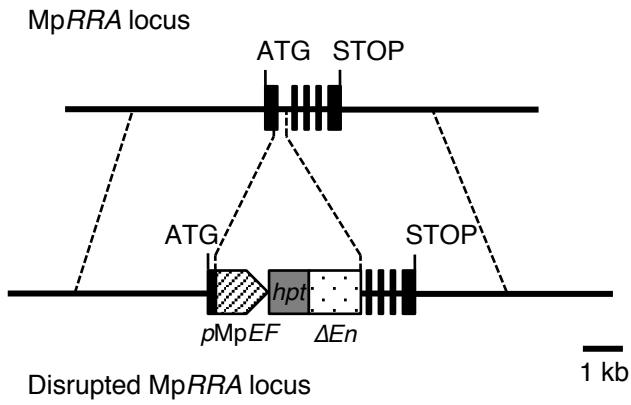
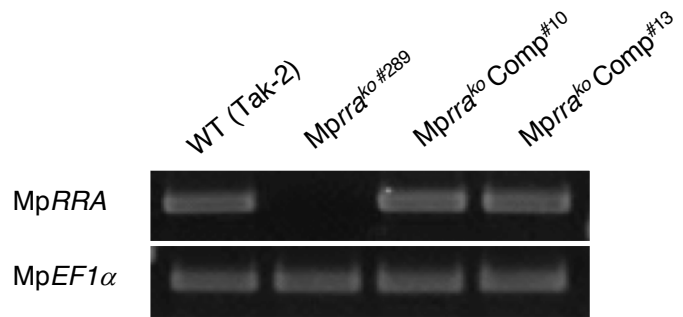


Fig. 5

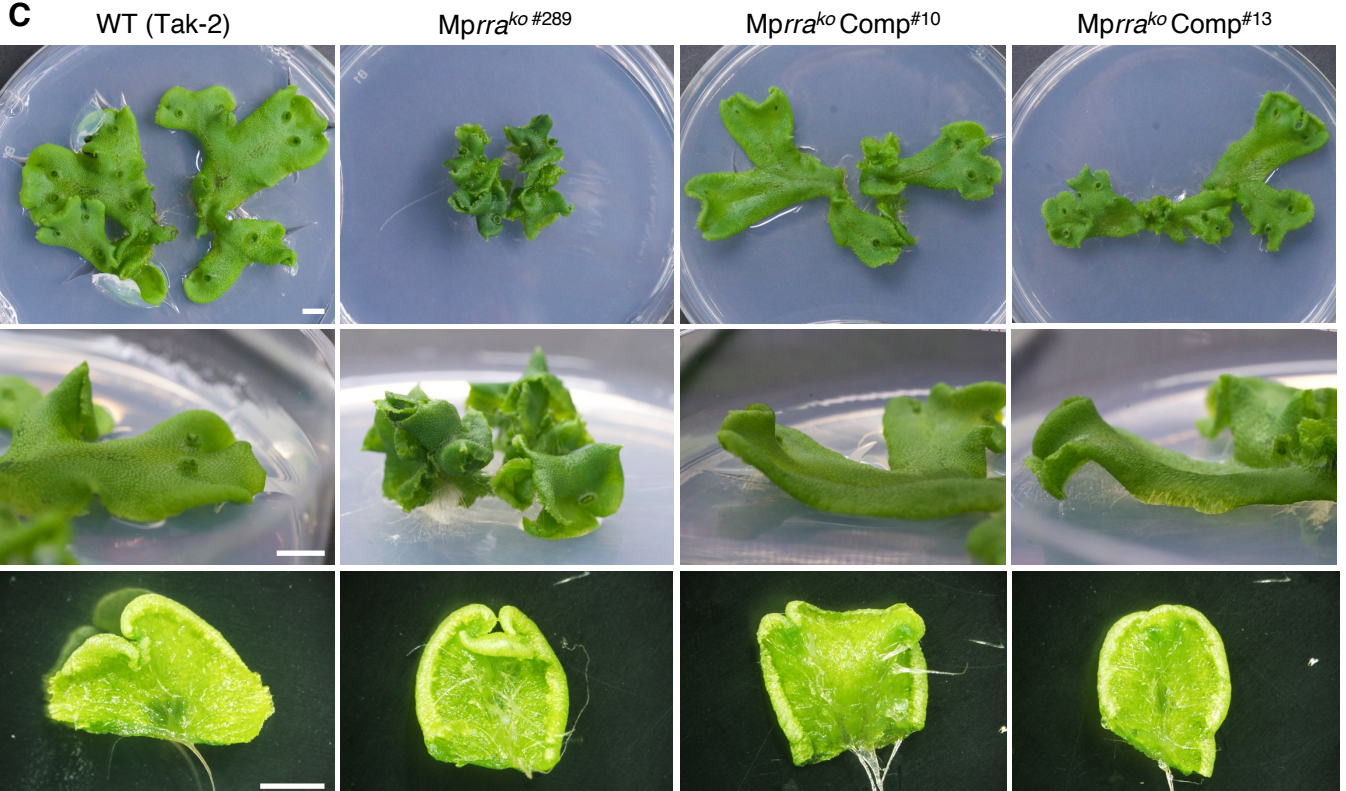
A



B



C



D

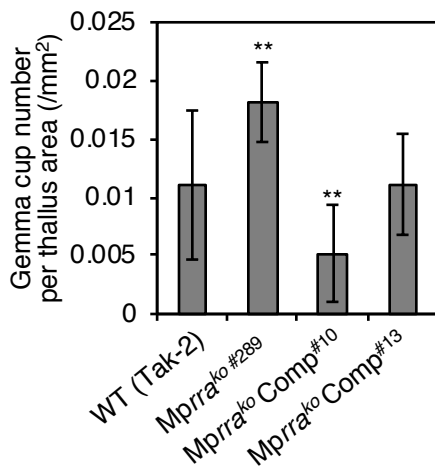


Fig. 6

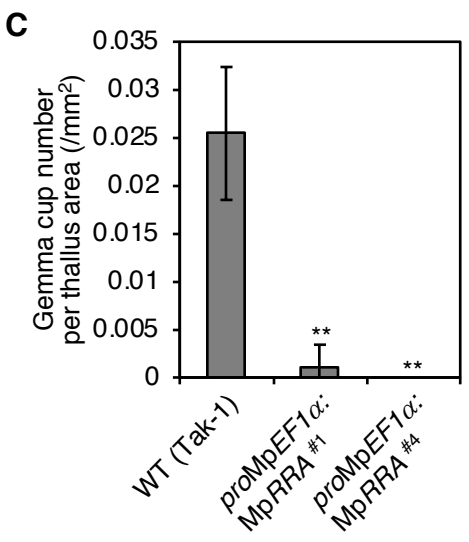
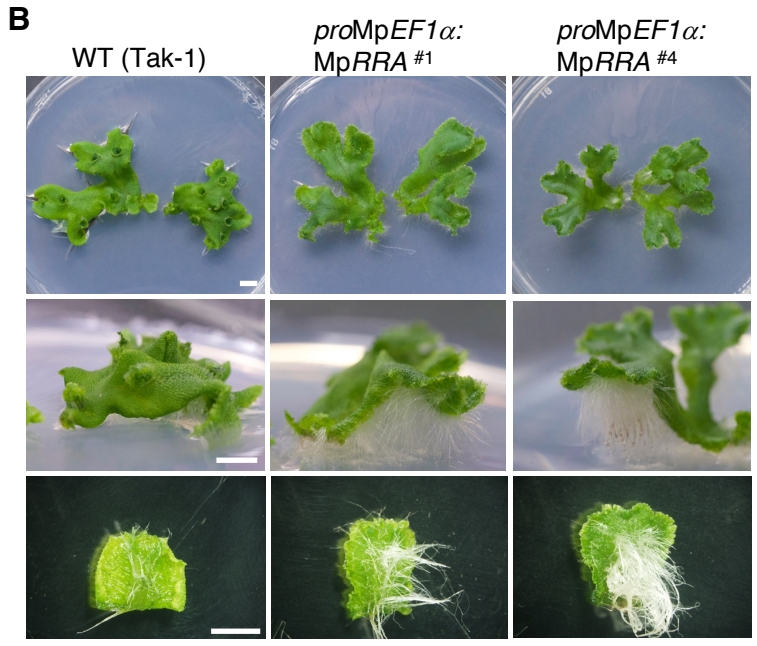
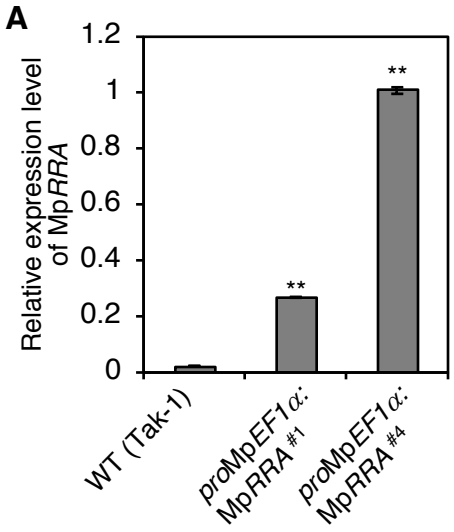
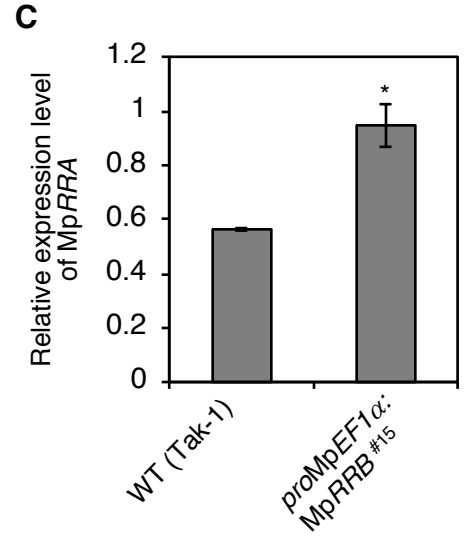
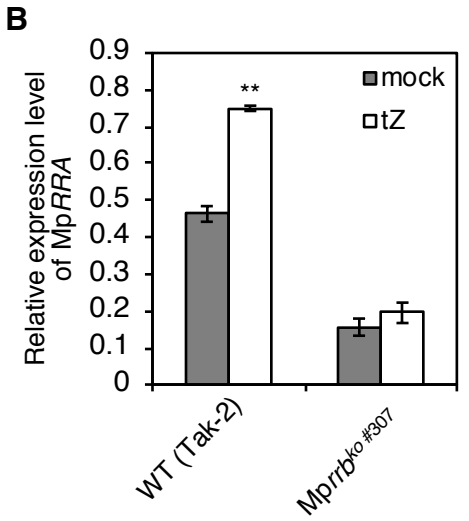
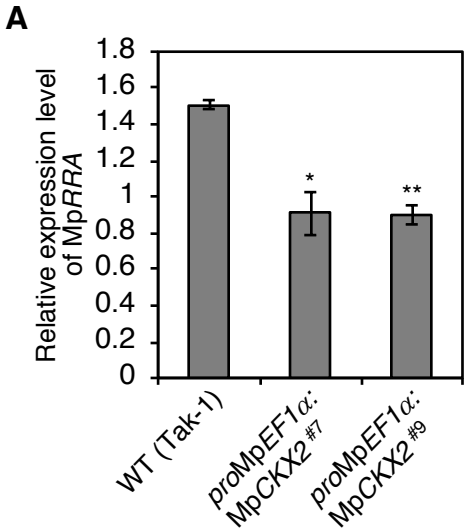


Fig. 7



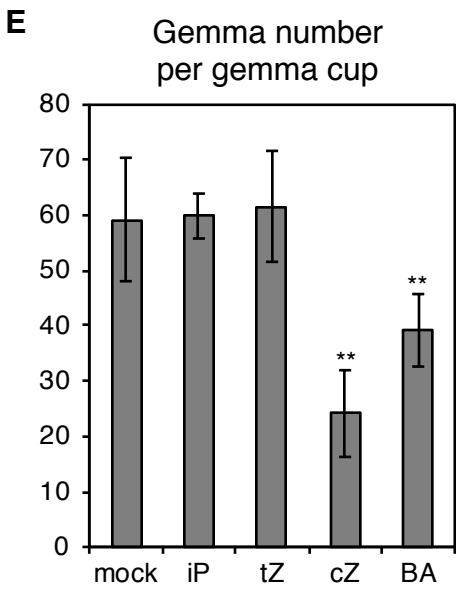
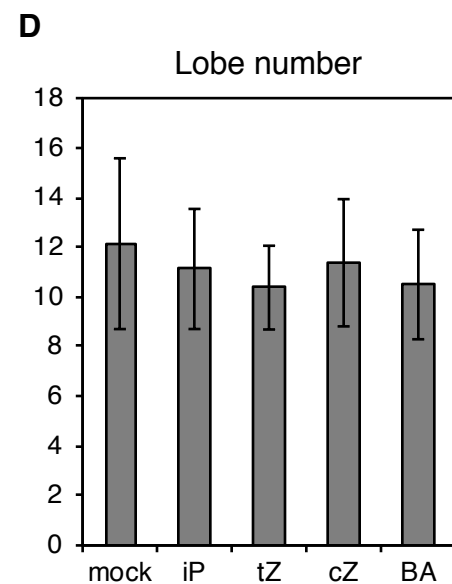
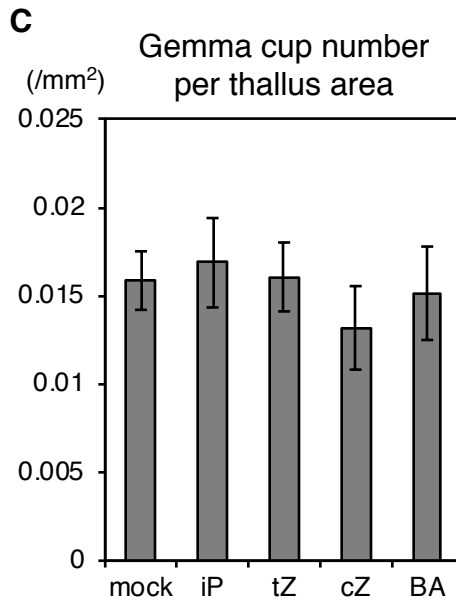
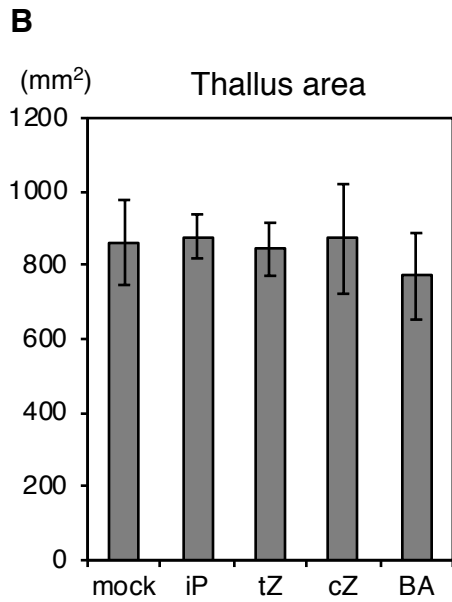
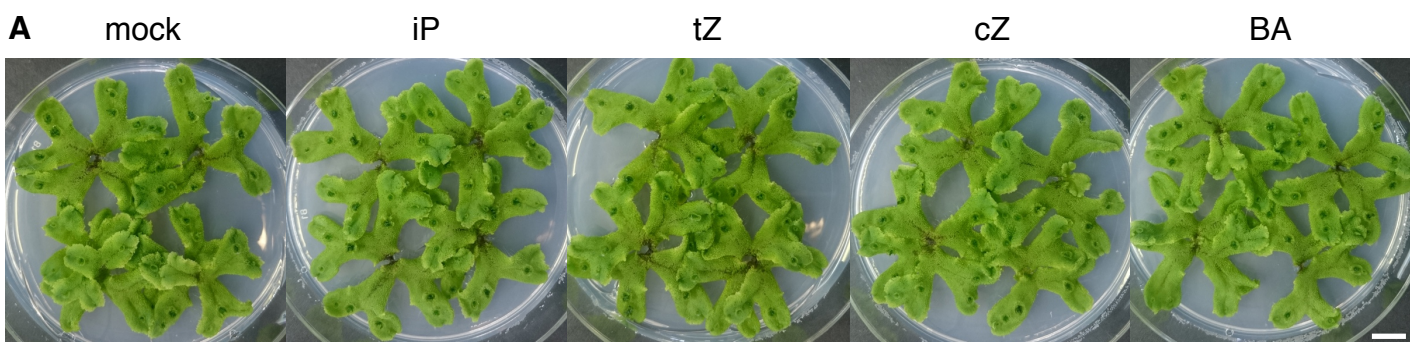


Fig. S1 Treatment of wild-type *Marchantia* (Tak-1) with 10 μ M cytokinins. Six-day-old plants were transferred to agar medium containing 10 μ M cytokinins, iP, tZ, cZ or BA, and cultured for 21 days. (A) Thalli of cytokinin-treated plants. Bar represents 1 cm. (B-E) Thallus area (B), gemma cup number per thallus area (C), lobe number (D) and gemma number per gemma cup (E) of cytokinin-treated plants. Data are presented as mean \pm SD ($n \geq 7$). Significant differences from the samples without cytokinin treatment (mock) were determined by Student's *t*-test: **, $P < 0.01$.

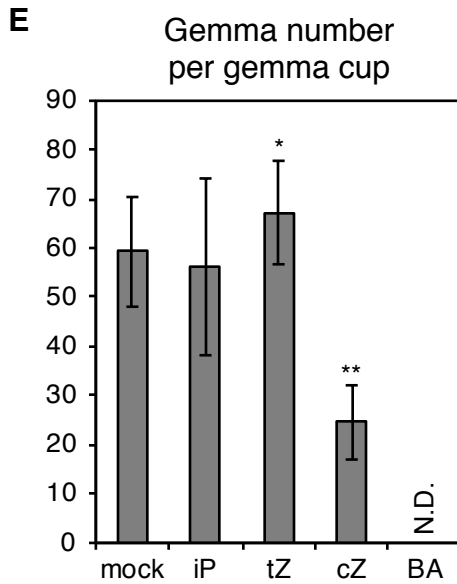
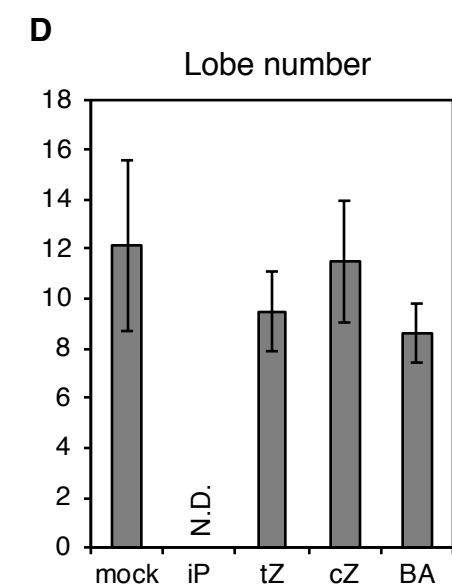
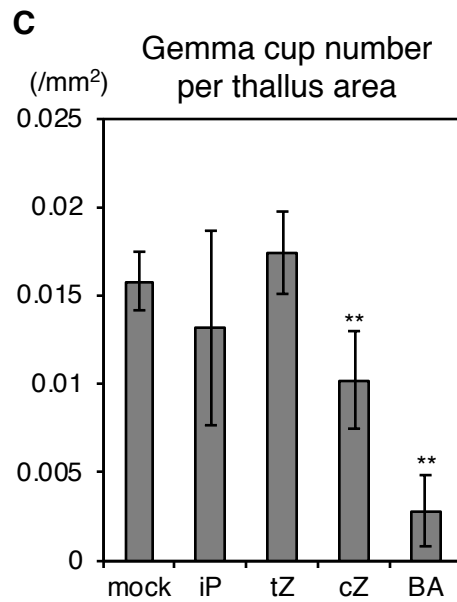
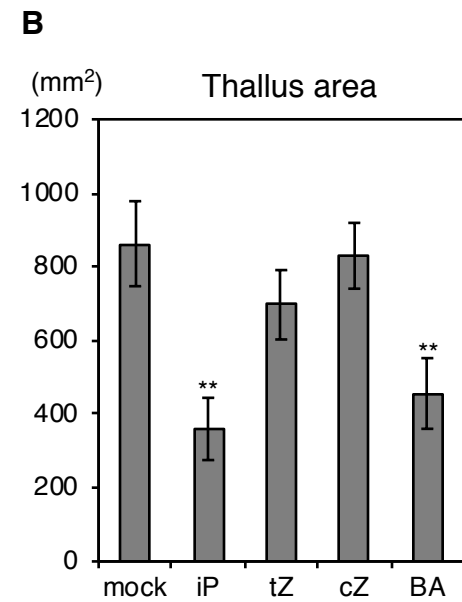


Fig. S2 Treatment of wild-type *Marchantia* (Tak-1) with 50 μ M cytokinins. Six-day-old plants were transferred to agar medium containing 50 μ M cytokinins, iP, tZ, cZ or BA, and cultured for 21 days. (A) Thalli of cytokinin-treated plants. Bar represents 1 cm. (B-E) Thallus area (B), gemma cup number per thallus area (C), lobe number (D) and gemma number per gemma cup (E) of cytokinin-treated plants. Data are presented as mean \pm SD ($n \geq 7$). Significant differences from the samples without cytokinin treatment (mock) were determined by Student's *t*-test: **, $P < 0.01$. N.D., not determined.

WT (Tak-1)

proMpEF1 α :
MpCKX2 #7

proMpEF1 α :
MpCKX2 #9

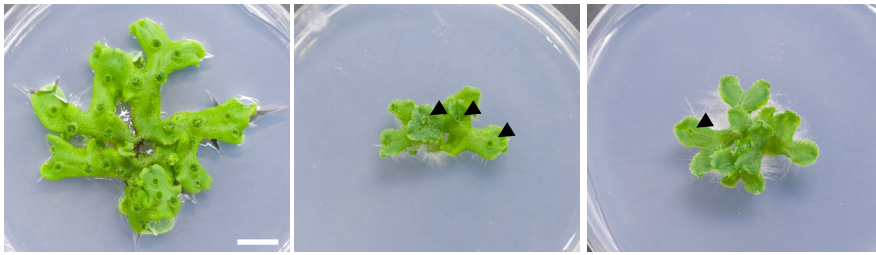


Fig. S3 *MpCKX2*-overexpressing lines #7 and #9. Gemmae were grown for 28 days. Arrowheads indicate gemma cups. Bar represents 1 cm.

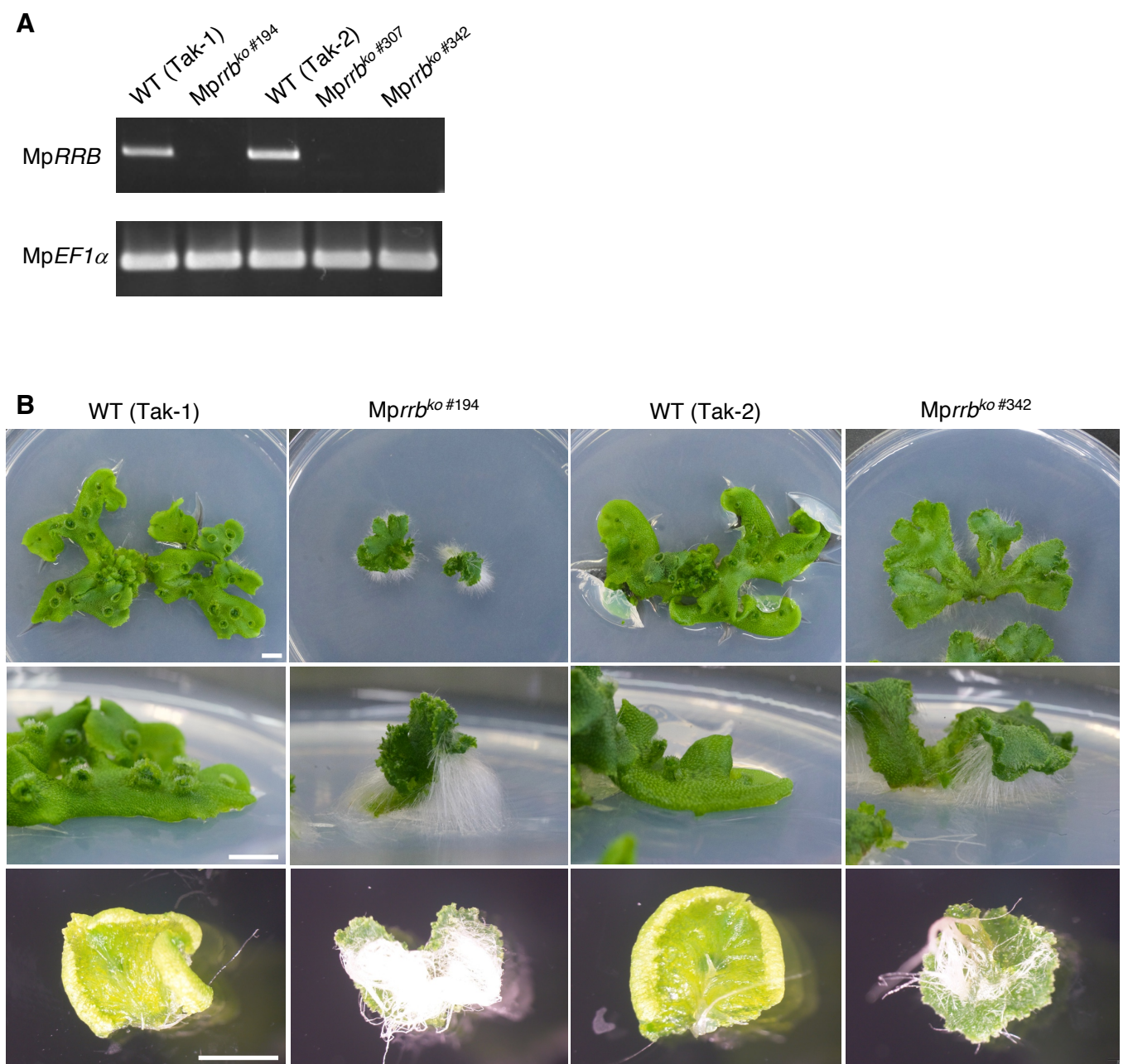


Fig. S4 *Mprrb* knockout lines #194 and #342. (A) *MpRRB* expression in *Mprrb* knockout lines. Semi-quantitative RT-PCR was performed using total RNA from the knockout lines #194, #307 and #342. *MpEF1 α* was used as a control. (B) Thalli and rhizoids of the *Mprrb* knockout lines. The pieces of thallus tip were cultured for 15 days. #194 and #342 have Tak-1 and Tak-2 backgrounds, respectively. Bars represent 5 mm.

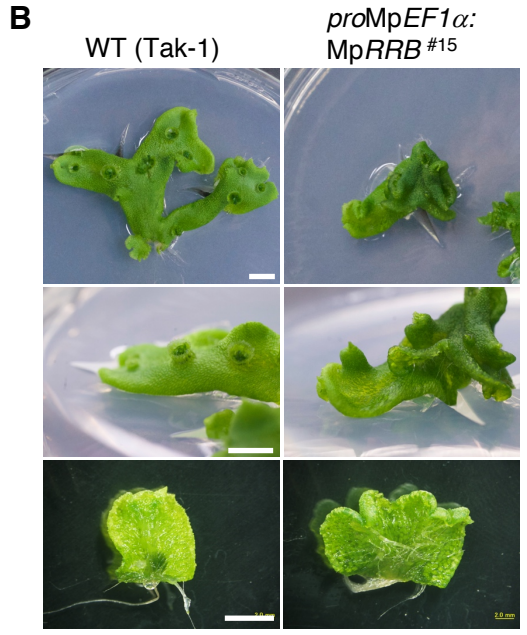
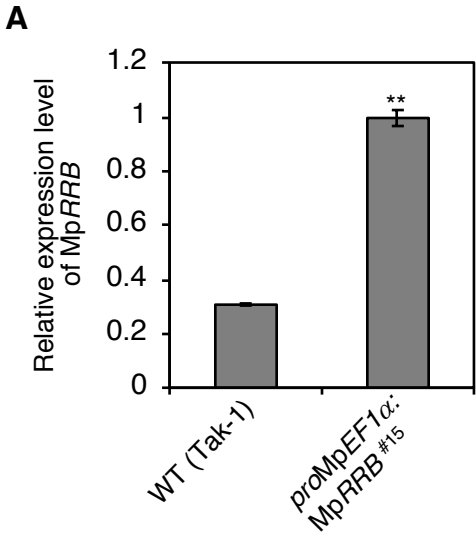


Fig. S5 Phenotype of the MpRRB-overexpressing line. (A) MpRRB expression in the MpRRB-overexpressing line #15. qRT-PCR was conducted using total RNA, and mRNA level was normalized to that of MpEF1a. Data are presented as mean \pm SD (n = 3). A significant difference from wild-type (Tak-1) was determined by Student's *t*-test: **, $P < 0.01$. (B) Thalli and rhizoids of the MpRRB-overexpressing line #15. The pieces of thallus tip were cultured for 15 days. Bars represent 5 mm.

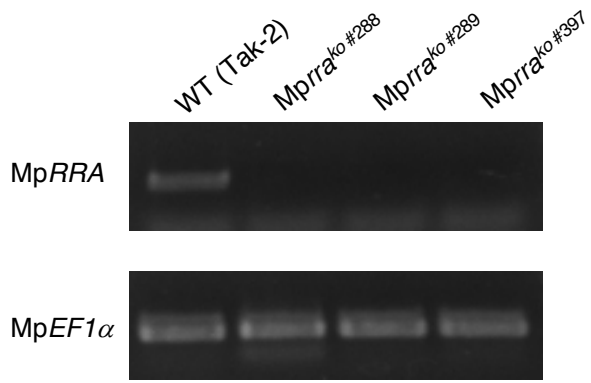
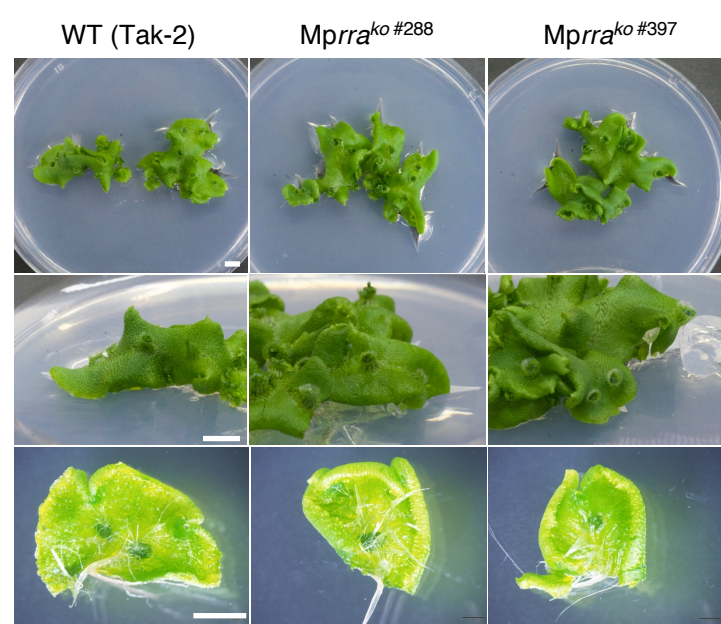
A**B**

Fig. S6 *Mprra* knockout lines #288 and #397. (A) *MpRRA* expression in *Mprra* knockout lines. Semi-quantitative RT-PCR was performed using total RNA from the knockout lines #288, #289 and #397. *MpEF1 α* was used as a control. (B) Thalli and rhizoids of the *Mprra* knockout lines. The pieces of thallus tip were cultured for 15 days. Bars represent 5 mm.

Supplementary Table S1. Primers used in this study

Experiment	Gene		Primer sequence (5' to 3')
Cloning of genes	MpRRA	cds	ATGCATGGGCGTTTCGAAGG TCAGGCAACGGTAAGCTCACTTA
	MpRRB	cds	ATGATGAAGTCATTTGATACAGC TCACTGACCCTGACCAGGCTAT
	MpRRA	promoter - stop codon	ATATCTACTTTTCTTGCAATAGAA TCAGGCAACGGTAAGCTCACTTA
	MpRRB	promoter - stop codon	ACTAGTCCTCTTACTTGGCT TCACTGACCCTGACCAGGCTAT
	MpCKX2	cds	ATGATGCTGCAATTACTGAAATATC TCATAATAGGAACGGGAATGTC
Cloning of promoters	MpRRA	promoter	ATATCTACTTTTCTTGCAATAGAA GCAGGGGAGCTGCCTGCG
	MpRRB	promoter	ACTAGTCCTCTTACTTGGCT GGACTCGCAACTAGACGTTC
Gene targeting	MpRRA	PacI site	ctaaggtagcgattaGACAAAGGAATGCAGTGCCGAATT gcccgggcaagcttaCTCTCTACGGTGTCCACCGAATT
		AscI site	taaactagtggcgcgGTTTGGCTTTCATCGAGTTTCTTGT ttatccctaggcgcgCAGAGGGCCGCAACCAATT
	MpRRB	PacI site	ctaaggtagcgattaTAGGCCTACGGCCCTACTCT gcccgggcaagcttaGCACTTTCAAACCAATGGGAGAAAA
		AscI site	taaactagtggcgcgCCCCTCATTAGTAAGTTATTTCCCCTTCT ttatccctaggcgcgCAGGAAGGCGATGATACACAAAATC
Semi-quantitative RT-PCR	MpRRA		ATGCATGGGCGTTTCGAAG TCAGGCAACGGTAAGCTCA
	MpRRB		ATGATGAAGTCATTTGATACAGCCA TCACTGACCCTGACCAGG
	MpEF1a		TCACTCTGGGTGTGAAGCAG GCCTCGAGTAAAGCTTCGTG
Quantitative RT-PCR	MpRRA		TCCCTGAAGGAAGTTCCAGTC CTTACGTCCTAGTTGCAC
	MpRRB		GGTTTGAAAGTGCTCGTTGTCTG AGGGAGAGAGCATCTACGGC
	MpCKX2		CCGTGGATTTTGGCCACATC TCACATTGGAGCTCGAGGC
	MpEF1a		AAGCCGTCGAAAAGAAGGAG TTCAGGATCGTCCGTTATCC